

UC Irvine

UC Irvine Electronic Theses and Dissertations

Title

Innovations in Centrifugal Microfluidics for Pathogen Detection in Water

Permalink

<https://escholarship.org/uc/item/61t7339r>

Author

Gowda, Hamsa Nandini

Publication Date

2021

Peer reviewed|Thesis/dissertation

UNIVERSITY OF CALIFORNIA,
IRVINE

Innovations in Centrifugal Microfluidics for Pathogen Detection in Water

DISSERTATION

submitted in partial satisfaction of the requirements
for the degree of

DOCTOR OF PHILOSOPHY

in Biomedical Engineering

by

Hamsa Nandini Gowda

Dissertation Committee:
Professor Marc Madou, Chair
Professor Sunny Jiang
Professor Abraham Lee

2021

DEDICATION

To

my family and friends

in recognition of their unconditional love, support, and encouragement over the last few years.

TABLE OF CONTENTS

	Page
LIST OF FIGURES	vi
LIST OF TABLES	viii
ACKNOWLEDGEMENTS	ix
VITA	xi
ABSTRACT OF THE DISSERTATION	xii
CHAPTER 1- INTRODUCTION: CHALLENGES IN PATHOGEN WATER QUALITY ANALYSIS	1
CHAPTER 2 – PORTABLE ANALYSIS SYSTEM FOR WATER QUALITY ANALYSIS	4
2.1 BACKGROUND	4
2.1.1 METHODS OF BACTERIAL DETECTION IN PATHOGEN WATER MONITORING	
2.1.2 MOLEULAR DIAGNOSTICS USED IN MICROFLUIDIC SYSTEMS	
2.1.3 NAAT-BASED PATHOGEN DETECTION ON CENTRIFUGAL MICROFLUIDIC SYSTEMS	
2.1.4 CURRENT LIMITATIONS AND PROPOSED METHOD OF PATHOGEN DETECTION IN WATER	
2.2 MATERIALS AND METHODS	9
2.2.1 MICROFLUIDIC FABRICATION AND ASSEMBLY	
2.2.2 BIOLOGICAL AND CHEMICAL REAGENT PREPARATION	
2.2.3 DESIGN OF ANALYSIS DEVICE	
2.3 RESULTS AND DISCUSSION	15
2.3.1 FLUIDIC INTEGRATION OF DDLAMP ASSAY ON-DISC	
2.3.2 EFFECTIVENESS OF ON-DISC SAMPLE PREPARATION	
2.3.3 ON-DISC DETECTION OF <i>E. FAECALIS</i> IN SPIKED DI WATER SAMPLES	
2.3.4 IMAGE PROCESSING AND QUANTIFICATION	

2.3.5 CHALLENGES AND LIMITATIONS	
2.4 CONCLUSIONS	28
CHAPTER 3 – SAMPLE CONCENTRATION SYSTEM FOR WATER QUALITY ANALYSIS	30
3.1 BACKGROUND	30
3.1.1 COMMON METHODS OF SAMPLE CONCENTRATION IN PATHOGEN WATER MONITORING	
3.1.2 SUPER ABSORBENT POLYMER BEADS FOR WATER SAMPLE CONCENTRATION	
3.1.3 CURRENT LIMITATIONS AND PROPOSED METHOD FOR WATER SAMPLE CONCENTRATION ON CENTRIFUGAL MICROFLUIDIC SYSTEM	
3.2 MATERIALS AND METHODS	33
3.2.1 SAMPLE CONCENTRATION SYSTEM FABRICATION AND ASSEMBLY	
3.2.2 BACTERIAL SAMPLE PREPARATION	
3.3 RESULTS AND DISCUSSION	35
3.3.1 INTEGRATION OF SAP BEADS ONTO CENTRIFUGAL MICROFLUIDIC PLATFORM	
3.3.2 ON-DISC CONCENTRATION OF <i>E. COLI</i> IN SPIKED DI WATER SAMPLES	
3.3.3 ON-DISC CONCENTRATION OF <i>E. COLI</i> IN SPIKED DI WATER SAMPLES USING DIFFERENT SAP BEAD SIZES	
3.3.3 ON-DISC CONCENTRATION OF <i>E. COLI</i> IN SPIKED DI WATER SAMPLES USING DIFFERENT ROTATION SPEEDS	
3.4 CONCLUSIONS	41
CHAPTER 4 – ASSAY DEVELOPMENT FOR ASSESSING PATHOGEN VIABILITY AND INFECTIVITY IN WATER	43
4.1 BACKGROUND	43
4.1.1 COMMON METHODS FOR ASSESSING VIABLE PATHOGENS IN WATER SAMPLES	
4.1.2 RNA AS A MARKER FOR ASSESSING VIABLE PATHOGENS	
4.1.3 SIGNAL AMPLIFICATION AND ENZYME-ASSISTED TARGET RECYCLING	

4.1.4 DUPLEX-SPECIFIC NUCLEASE	
4.1.5 DSN-MEDIATED STRATEGY FOR SPECIFIC BACTERIAL DETECTION	
4.1.6 DSN-MEDIATED STRATEGY FOR VIABLE BACTERIAL DETECTION	
4.1.7 DSN-MEDIATED STRATEGY DETECTION PLATFORM VERSATILITY	
4.2 MATERIALS AND METHODS	50
4.2.1 BACTERIAL SEQUENCE AND PROBE DESIGN	
4.2.2 PLATFORM DESIGN	
4.2.3 IMMOBILIZATION PROTOCOL	
4.2.4 HYBDRIDIZATION PROTOCOL	
4.2.5 DSN-MEDIATED TARGET RECYCLING PROTOCOL	
4.3 RESULTS AND DISCUSSION	53
4.3.1 IMMOBILIZATION EFFECIENCY	
4.3.2 HYBRIDIZATION EFFICIENCY	
4.3.3 FEASIBILITY OF DSN-MEDIATED STRATGEY	
4.4 CONCLUSIONS	58
CHAPTER 5 – CONCLUSIONS AND FUTURE WORK	60
BIBLIOGRAPHY	62

LIST OF FIGURES

	Page
Figure 1. Assembly and fabricated ddLAMP disc	10
Figure 2. Schematic and fabricated analysis device	13
Figure 3. Disc design and fluidics depicting main steps of ddLAMP assay	17
Figure 4. Fluidic integration and confirmation on-disc lysis, centrifugation, extraction, and metering	22
Figure 5. Fluidic integration and confirmation of mixing on-disc	23
Figure 6. On-disc ddLAMP amplification results	24
Figure 7. ddLAMP image processing	25
Figure 8. Droplet stability during heating	27
Figure 9. Temperature feedback during amplification	28
Figure 10. Assembly and fabricated sample concentration device	34
Figure 11. Schematic of sample concentration device workflow	36
Figure 12. Comparison of on-disc and stationary concentration method	38
Figure 13. Compatibility of different SAP bead sizes with sample concentration device	39
Figure 14. Comparison of rotation speeds using sample concentration device	41
Figure 15. Basic enzyme-assisted target recycling scheme	45
Figure 16. DSN-mediated signal amplification scheme	46
Figure 17. DSN-mediated strategy for sequence-specific detection	47
Figure 18. Integration of DSN-mediated strategy with modified culture assay	49
Figure 19. Immobilization Efficiency	54
Figure 20. Hybridization Efficiency	55
Figure 21. Effect of sequence on immobilization and hybridization	56

Figure 22. Feasibility of DSN-mediated target recycling signal amplification	57
Figure 23. Effect of time and DSN concentration on signal amplification	58
Figure 24. Integration of DSN-mediated assay onto centrifugal microfluidic disc	59

LIST OF TABLES

	Page
Table 1. LAMP Primers	11
Table 2. Mastermix Components	12
Table 3. Step-by-step Protocol for ddLAMP Assay on-disc	21
Table 1. Selected Bacterial Sequences for Capture and Target Probes	51

ACKNOWLEDGEMENTS

I would like to acknowledge my committee chair, Dr. Marc Madou for taking me under his wing as a graduate student, giving me various different opportunities in academia and industry to grow as engineer, and offering both his scientific expertise, humor, and kindness. I also want to thank Dr. Sunny Jiang who was an integral advisor in my PhD journey and provided me with guidance, encouraged my scientific curiosity, and support during the hard times. I would like to acknowledge my committee members, Dr. Abraham Lee, Dr. Jered Haun, and Dr. Oladele Ogunseitan for their scientific guidance during the qualifying exam and help over the past few years.

I would like to thank my labmates and undergraduates in both the Madou and Jiang lab for their inspiring scientific curiosity and determination, and on-going support and contributions both in and out of the lab. I would like to acknowledge the Biomedical Engineering Department, Graduate Association for Biomedical Engineering Students, and Association for Women in Science, GPS-STEM, and Research Translation Group at UCI Beall Applied Innovation for creating spaces and opportunities for me to meet life-long friends, create a community, and explore career opportunities.

I would like to acknowledge my hometown friends from childhood and college for their unwavering support and encouragement during every visit home. I would like to thank my significant other, Neil Patel, for his humor, understanding, and positive attitude toward life which has truly helped me through the challenges over the years and pushed me to grow as a person. Finally, I would like to thank my mom, dad, sister, brother-in-law, niece and nephew for their unconditional love, support, and putting their trust in me to move across country and attend graduate school. I am deeply grateful to have you all in my life.

Finally, I would like to acknowledge my funding sources various parts of my dissertation which include the Bill and Melinda Gates Foundation OPP1111252 and National Institutes of Health (NIH) under Prime Award no. UL1 TR001414.

VITA

Hamsa Nandini Gowda

Education

- 2014 B.S. in Chemical Engineering, University of Maryland, Baltimore County
- 2018 M.S. in Biomedical Engineering, University of California, Irvine
- 2020 Ph.D. in Biomedical Engineering, University of California, Irvine

Honors

- 2018-2019 UCI Public Impact Fellow
- 2018-Present UCI Beall Applied Innovation Research Translation Group Fellow

Experience

- 2015-2020 Graduate Student Researcher, UC Irvine
- 2017-2020 Teaching Assistant, UCI Biomedical Engineering Department
- 2017-2018 Research Consultant, Nexus Dx, Inc.
- 2019-2020 Graduate Studies Committee Engineering Student Representative, UCI Engineering Department

Extracurricular Activities

- 2017-2020 Vice President, Outreach, UCI Graduate Association for Biomedical Engineering Students
- 2019-2020 Social Chair, UCI Association for Women in Science

Publications and Patents

Jiang, Sunny, Hamsa Gowda, Xiao Huang, Xunyi Wu, Marc Madou, and Michael R. Hoffmann. "Portable pathogen analysis system for detecting waterborne pathogens." U.S. Patent Application 16/153,423, filed April 11, 2019.

Suh, Youngjoon, Cheng-Hui Lin, Hamsa Gowda, and Yoonjin Won. "Multiscale Evaporation Rate Measurement Using Microlaser-Induced Fluorescence." *Journal of Electronic Packaging* 142, no. 3 (2020).

Suh, Youngjoon, Hamsa Gowda, and Yoonjin Won. "In situ investigation of particle clustering dynamics in colloidal assemblies using fluorescence microscopy." *Journal of Colloid and Interface Science* (2020).

ABSTRACT OF THE DISSERTATION

Innovations in Centrifugal Microfluidics for Pathogen Detection in Water
by

Hamsa Nandini Gowda

Doctor of Philosophy in Biomedical Engineering

University of California, Irvine, 2021

Professor Marc Madou, Chair

Waterborne diseases cause millions of deaths worldwide, especially in developing communities. The detection of waterborne pathogens is a critical step for the selection of water treatment processes that will lead to the prevention of disease transmission. Unfortunately, analyzing water samples is a lengthy and laborious process that requires 1) collecting and transporting large volumes of samples (>1 L) to a centralized lab, 2) sample preparation for downstream analysis, 3) using appropriate detection methods to identify pathogens and 4) estimating the proportion of viable pathogens that pose a risk to public health. This lengthy “sample-to-answer” process significantly delays the risk mitigation actions, and subsequently exposes those using the water for daily necessities to pathogen infection. This dissertation aims to streamline the water sample analysis timeline by incorporating the major laboratory steps onto centrifugal microfluidic platforms for implementation at the point-of-sample collection, mitigating many of the aforementioned limitations. We first investigate pathogen detection methods by describing the integration of a droplet digital loop mediated isothermal DNA amplification assay onto a centrifugal microfluidic disc that coupled with a portable analysis instrument, can detect *E. faecalis*, a common waterborne pathogen. We highlight the fluidic and functional integration of the major steps of the assay onto the disc as well as the rapid, quantitative, hands-free aspects of the system. Next, to process samples in our detection system, we tackle upstream sample

preparation by focusing on adopting simple and accessible water sample concentration mechanisms onto a centrifugal microfluidic platform. We integrate super absorbent polymer beads with the disc system to concentrate *E.coli*, another common waterborne pathogen, and observe how the concentration is affected by various relevant parameters. We conclude by discussing strategies for downstream assessment of pathogen viability and relevant infectivity in water samples. We describe the method and initial feasibility of a RNA-based, enzyme-mediated signal amplification strategy to detect *E.coli* and highlight its integration into modified culture-based assays for rapid, viable pathogen detection and risk assessment. Together, this work highlights the critical challenges in water analysis and innovations in centrifugal microfluidics for pathogen detection at the point-of-sample collection.

CHAPTER 1

INTRODUCTION: CHALLENGES IN PATHOGEN WATER QUALITY ANALYSIS

Lack of proper sanitation, hygiene, and water supply has increased the potential of contamination and health risk in much of the developing world. The World Health Organization (WHO)/United Nations Children's Fund (UNICEF) Joint Monitoring Programme for Water Supply, Sanitation, and Hygiene (WASH) tracks the progress of these areas on an international scale. From the 2019 update, they estimated that 29% of the global population (2.2 billion people) and 40% (3 billion people) did not have access to safe drinking water or proper handwashing supplies at home, respectively, and 55% of the global population (4.2 billion people) did not have access to a toilet with proper waste disposal methods in 2017 ("Water Supply, Sanitation And Hygiene Monitoring", 2020). Unfortunately, these unsafe WASH conditions can lead to the spread of waterborne pathogens and ultimately to outbreaks of diarrhea, infections, gastrointestinal diseases and death in severe cases (Ramírez-Castillo et al., 2015; van Seventer, and Hochberg, 2017). In developing areas where communities share single water sources or sanitation systems and the increasing popularity around water reuse, environmental water quality monitoring is more critical than ever. Wastewater has a variety of contaminants that range from microbial pathogens to chemical hazards. As a result, both treatment and monitoring of wastewaters is critical to public health to prevent continued spread and contamination.

Microbial hazards denoted by WHO in wastewater include viruses, bacteria, protozoa and helminths. Bacteria, specifically, include *Escherichia coli*, *Enterococci*, *Clostridium perfringens*,

Campylobacter, *Salmonella*, *Shigella*, and *Vibrio cholerae*. Fecal indicator bacteria, namely *Escherichia coli* and *Enterococci*, have been used in part to assess the quality of water and presence of potential pathogens. *E.coli* has become the more prominent indicator because its detection methods are fast, simple, and more sensitive and specific compared to the others (Odonkor, and Ampofo, 2013). However, the EPA recommends using *Enterococci* as the main indicator in marine and brackish waters as evidence has shown it has a better correlation to health effects (Byappanahalli et al., 2012).

Detection of these bacteria has seen recent improvements in molecular diagnostics such as nucleic acid amplification techniques (NAAT) which has significantly advanced the speed, sensitivity, and specificity in clinical, food safety, and environmental samples, over traditional systems such as cultivation, microscopy, and immuno-based tests (Platts-Mills et al., 2011; Rajapaksha et al., 2019). From the original method of amplification using the polymerase chain reaction (PCR) method, numerous amplification methods have followed including reverse-transcriptase PCR (RT-PCR), quantitative PCR (qPCR), isothermal amplification methods, and more recently, digital amplification techniques. More specifically, digital nucleic acid amplification has allowed for direct quantification of the target concentration in a binary format after amplification (Hindson et al., 2011; Sanders et al., 2011; Pinheiro et al., 2011; Quan et al., 2018).

However, these methods are still mainly confined to air-conditioned, well-equipped laboratory settings where trained technicians and expensive reagents are required (Platts-Mills et al., 2011; Ramírez-Castillo et al., 2015; Rajapaksha et al., 2019). Environmental water samples, specifically, require extra steps to filter contaminants and concentrate large volumes to achieve a detectable pathogen concentration. The near real-time sample-to-answer diagnosis that is needed

to stop the spread of infectious disease is therefore significantly lengthened due to the need for sample preservation, transport after collection, sample preparation, and assay time (Ramírez-Castillo et al., 2015; Jofre & Blanch, 2010) . In recent years, some of the downstream techniques have been implemented onto microfluidic platforms. These platforms enable many benchtop processes, such as cell lysis, reagent mixing, heating, etc. to occur within microscale volumes and the design also allows some degree of automation, minimizing the need for expensive equipment and trained professionals (Sia & Kricka, 2008). Despite these advantages, some still lack the full integration of sample preparation, reactions, detection, and risk assessment that is needed for implementation in developing areas with minimal infrastructure and financial resources. Within microfluidics, centrifugal-based systems offers the ability to integrate these processes on a disc-shaped chip without the need for external valving and pumps by using the pseudo forces (centrifugal, Coriolis, Euler) and non-pseudo (viscous, pneumatic, capillary, fluidic inertia) present during rotation to manipulate and drive fluid motion. As a result, these discs have been heavily used for clinical diagnostics and leveraged for point-of-care settings (Strohmeier et al., 2015; Kong et al., 2016; Tang et al., 2016; Smith et al., 2016). However, centrifugal microfluidics has been limited in its use in the environmental realm especially with respect to pathogen detection in water (Maguire et al., 2018). Due to this gap, we investigate how major steps needed for assessing pathogens and risk in water samples can be integrated into centrifugal microfluidic platforms for use at the point-of-sample collection.

CHAPTER 2

PORTABLE PATHOGEN ANALYSIS SYSTEM FOR WATER QUALITY ANALYSIS

2.1 Background

2.1.1 Methods of Bacterial Detection in Pathogen Water Monitoring

Detection of bacteria in water samples with common clinical detection methods are used, but can be tricky due to the inherent low concentrations and presence of many possible inhibitors in natural waters (Ramírez-Castillo et al., 2015). Fecal indicator bacteria, total and fecal coliforms, *E.coli* and *Enterococci*, have been used to assess the presence of other potential pathogens in the water. The Environmental Protection Agency (EPA) and WHO put a specific emphasis on using *E.coli* for drinking water, bathing/recreational water, and *Enterococci* for marine and bathing/recreational waters (Mendes Silva, and Domingues, 2015). The EPA, WHO, and European Union (EU) additionally have the following requirements for *E.coli* and *Enterococci* in drinking and recreational waters: 1) There should be no present *E. coli* and *Enterococci* in 100 mL of water for human consumption or in 250 mL of bottled drinking water and 2) the level of *E.coli* should not exceed $2 \log_{10}$ units/100 mL and the level of *Enterococci* should not exceed $1-2_{\log_{10}}$ units/100 mL in recreational waters (Jofre and Blanch, 2010). Methods approved by EPA for detection of microbial pathogens in wastewater, sewage sludge, and ambient water include membrane filtration followed by culture (specific to bacteria type) ("Approved CWA Microbiological Test Methods | US EPA", 2020). Although these methods have been established, the EPA does work with other entities that are utilizing methods such as PCR. For example, the EPA has supported qPCR for use in rapid detection of *Enterococcus spp*

in recreational waters ("Other Clean Water Act Test Methods: Microbiological | US EPA", 2020; Kolm et al., 2017). Aside from EPA regulations and developing methods, researchers have been investigating other methods such as variations of PCR, fluorescent in situ hybridization (FISH), immuno-based methods, biosensors, microarrays, and pyrosequencing (Lebaron et al., 2005).

Of the molecular techniques, nucleic acid amplification techniques (NAATs) have improved molecular diagnostic sensitivity enabling more rapid, real-time monitoring with a quantitative approach (e.g. quantitative PCR, digital NAAT). In the general nucleic acid amplification scheme, primers that are complementary to sequences in your target DNA or RNA are mixed in with your bulk sample and allowed to anneal; with the help of specific enzymes (e.g., DNA Polymerase) and optimized conditions (e.g. temperature cycling, buffers, etc.) the reaction causes the target sequences to grow and multiply, resulting in an exponential amplification after many cycles. In more quantitative approaches such as digital DNA amplification, the bulk sample is divided equally into many microreactors by way of structural microwells or through generating droplets or emulsions. Based on Poisson statistics, each reactor ideally contains at least 1 or 0 DNA molecules at the start of the reaction and as the cyclical reaction is initiated, the target DNA molecules in each "microreactor" are amplified following the same principles in the traditional DNA amplification scheme. In optical detection platforms where fluorescent dyes can be intercalated with the amplification products, the resulting positive (fluorescent), negative (not-fluorescent) droplets, and total droplets can be counted and fitted to a Poisson distribution to determine the concentration (Hindson et al., 2011; Sanders et al., 2011; Pinheiro et al., 2011; Quan et al., 2018). PCR was the first of the NAAT to be executed in this format, however, isothermal amplification techniques have followed suit. Digital loop mediated isothermal amplification (dLAMP) follows this sample principle but is performed at one

temperature (65 °C) and uses four to six primers instead of two as in PCR. Although traditional LAMP relies on qualitative detection through fluorescence or calorimetric inspection of a sample after amplification, dLAMP provides a quantitative result with high specificity sensitivity without the need for temperature cycling (Yuan et al., 2020).

However, all of these aforementioned molecular methods as well as traditional methods such as culturing and microscopy, require the use of laboratory material, equipment, long lag-times (depending on the method), and have varying sensitivities and correlations with health risk (Platts-Mills et al, 2011; Ramírez-Castillo et al., 2015; Rajapaksha et al., 2019). In developing areas where water quality information is time-sensitive, these lengthy procedures cause a delay in information and increased health risks.

2.1.2 Molecular Diagnostics used in Microfluidic Systems

Microfluidic systems are an attractive format for molecular diagnostics, especially nucleic acid amplification techniques. The goal of microfluidic systems is to miniaturize, automate, and streamline many of the benchtop processes and complicated assays to reduce time, volume, and labor to ensure reproducibility, high sensitivity, and quick turnaround times. Many have been utilized for assessing clinical samples including detecting foodborne pathogens on microfluidic chips (Tourlousse et al., 2012; Duarte et al., 2013; Tang et al., 2016), Mycobacterium tuberculosis in a microcapillary system (Liu et al., 2013), HIV and HCV using SlipChip technology, (Shen et al., 2011; Xia et al., 2016). Additionally, this research has led companies such as Fluidigm Corporation, Life Technologies, RainDance Technologies, and Bio-Rad to develop commercial systems based on microfluidics and partition methods to create droplets and perform digital PCR assays; however, in these systems the cost is high and there is

limited integration with upstream sample preparation ("Digital PCR: A Technical Guide To PCR Technologies", 2020).

Centrifugal microfluidics, a specific microfluidic platform, has also been utilized for molecular diagnostics and specifically nucleic acid amplification assays (Safavieh et al., 2016). On this platform, the fluidic design is created on a circular disc which spins on a rotor; this rotation creates pseudo forces and non-pseudo forces, which in turn help to pump the liquid from the center towards the outer perimeter of the disc. In conjunction with the fluidic design, the speed, and acceleration of rotation can be uniquely controlled to pump fluids through channels and chambers to different locations on the disc at specific time points. As a result, the Lab-on-Disc platform enables multiple units such as cell lysis, mixing, metering, valving, centrifugation, particle sorting, droplet generation and biochemical reactions to be employed on a disc through unique designs and automation (Strohmeier et al., 2015; Kong et al., 2016; Tang et al., 2016; Smith et al., 2016).

2.1.3 NAAT-based Pathogen Detection on Centrifugal Microfluidics Systems

Several key steps in the assay workflow of NAAT- based molecular diagnostics for have been investigated independently on the centrifugal microfluidic disc platform. With the help of magnetic actuation, a simulated bead- beating cell lysis technique has been developed on the disc (Kido et al., 2007). Loop-mediated isothermal assays for detection of pathogens (e.g., *E. coli*, *Salmonella*, etc.) have been incorporated onto the disc with a calorimetric or turbidity end-point analysis (Sayad et al., 2016; Yan et al., 2017; Ko, and Yoo, 2018). Some have included real-time LAMP capabilities to monitor fluorescence of the sample at specific timepoints throughout the reaction (Santiago-Felipe et al., 2016; Kinahan et al., 2018), while others have included individual chambers packed with pathogen-specific reagents to simulate the high-throughput

capabilities or multiplexing on the disc (Santiago-Felipe et al., 2016; Seo et al., 2017). Schuler et al utilized centrifugal step emulsification to create droplets on a disc which led to ability of performing digital droplet and Recombinase Polymerase Amplification to detect *Listeria monocytogenes* and digital droplet PCR to detect cystic fibrosis causing mutation p.Phe508del (Schuler et al., 2015; Schuler et al 2016).

2.1.4 Current Limitations and Proposed Method for Pathogen Detection in Water

Despite the development of several individual steps of NAAT assays on the disc platform, the major limitation of these devices lies in the lack of full integration of these steps into a complete assay from sample collection to quantitative end-point result without intermittent use handling and real-time monitoring. Additionally, many of these devices are tailored to laboratory or clinical samples which do not necessarily include factors that affect environmental samples (low concentrations, inhibitors etc.). A recent review highlighted the lack of environmental monitoring applications on this platform (Maguire et al., 2018), and of the limited applications, many have focused on monitoring of chemicals and toxins (Maguire et al., 2017; Meng et al., 2017; Zhu et al., 2017; Duffy et al., 2017; Duffy et al., 2017; Duffy et al., 2018) rather than pathogen detection in water.

Therefore, to adhere to water quality regulations and ensure safety of water for sanitation, hygiene, and drinking in both developed and developing countries, there is a great need for an integrated device that is rapid, portable and quantitative for analyzing pathogens in water at the point-of-sample collection. This chapter will focus on the development an integrated centrifugal microfluidics system for detection of waterborne pathogens utilizing a NAAT-based technique. In order to decrease complexity and provide absolute quantification, a digital droplet

LAMP assay is proposed, and the major assay steps are designed, integrated, and demonstrated using this platform.

2.2 Materials and Methods

2.2.1 Microfluidic Fabrication and Assembly

The microfluidic disc (Fig 1) is consists of four main layers: a bottom (3.2 mm thick) black polycarbonate (McMaster-Carr) disc with major chambers and channels, two biocompatible adhesive middle layers (150 μm joint thickness) (3M and Flexmount) consisting of the remaining connecting channels, and a top (1 mm) transparent polycarbonate disc with inlet and vent holes (Figure 1a). The design was created in SolidWorks with all microfluidic units (cell lysis, DNA extraction, reagent mixing, droplet generation, amplification, detection) integrated to fit on a disc with an outer diameter of 120 mm. The polycarbonate base is milled on a CNC machine (Tormach PCNC 440). The adhesive microfluidic channels are cut using a vinyl cutter (Silhouette CAMEO 2). A roller press is used to seal all the layers together.

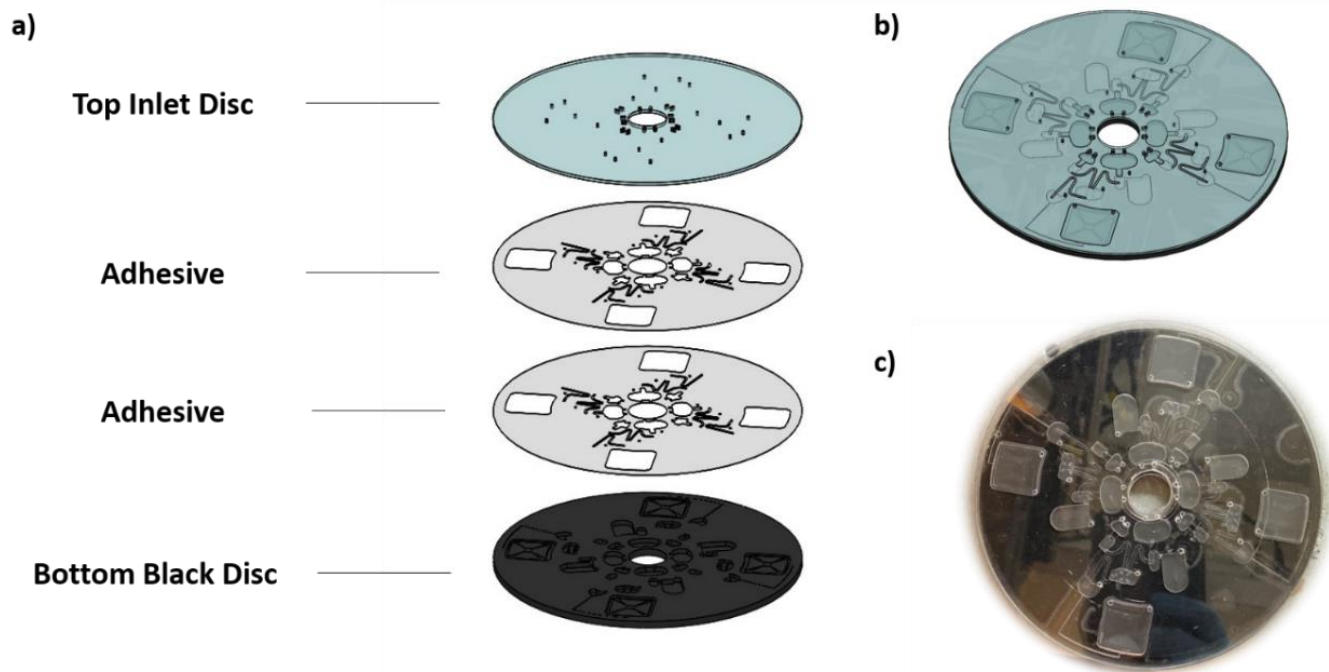


Figure 1. Solidworks illustration of a) four main layers of integrated disc and b) the assembled disc. c) image of actual fabricated and assembled prototype disc

2.2.2 Biological and Chemical Reagent Preparation

E. faecalis (ATCC 29212), a fecal bacterium that is commonly monitored to indicate the presence of enteric pathogens in water, was used as the target bacteria to demonstrate the proof-of-concept integrated ddLAMP assay on-disc. *E. faecalis* was cultured in Luria Bertaini (LB) broth at 37°C overnight. The culture was serially diluted in DI water and plated on LB agar plates to count colonies to estimate concentrations for comparison with the molecular detection method on the microfluidic disc

The mastermix for the LAMP reaction was consisted of the WarmStart 2X LAMP Master Mix with fluorescence dye (New England BioLabs) and the primers (IDT) targeting the *azoA* gene of *E. faecalis* with the amplicon size of 220 BP. The LAMP primers for *E. faecalis*

detection adopted from a previous study (Kato et al., 2007). The primers and their corresponding concentrations used in the mastermix are in Table 1.

Table 2. LAMP Primers

Primer	Sequence
F3 (0.2 μ M)	5'-GCCGGAAATCGATGAAGA-3'
B3 (0.2 μ M)	5'-TCCAGCAACGTTGATTGT-3'
FIP (1.6 μ M)	5'-CACTTTTTGTTGTTGGTTTTCGCTTTATTATCTGCTTGGGGTGC-3'
BIP (1.6 μ M)	5'-ATCTGCAGACAAAGTAGTAATTGCTCCAAGCTTTTAAGCGTGTC-3'
LoopF (0.8 μ M)	5'-AAATGCTGCGCCAGCTCG-3'
LoopB (0.8 μ M)	5'-TCCAATGTGGA ACTTAAACGTACC-3'

The Mastermix totals 23 μ L and the components and corresponding volumes is based on New England BioLabs protocol and is shown in Table 2.

Table 2. Mastermix Components

Mastermix	Amount/Concentration
Bst 2.0 WarmStart DNA polymerase and LAMP buffer solution (NEB)	12.5 μ L
Primer Mix (IDT)	2.5 μ L
Fluorescent Dye (NEB)	0.5
Molecular Biology Grade Water	7.5 μ L
Total	23 μ L

The Novec HFE 7500 oil (3M) was mixed with 5 wt % Fluor-surfactant (RAN Biotechnologies, Inc) to serve as the carrier for generation of reaction-in-oil droplets. BioRad PCR MasterMix and their proprietary oil were initially used for fluidic testing and troubleshooting. Specific valves (siphon channels) were coated with Casein (ThermoFisher Scientific) to increase the hydrophilicity of the polycarbonate surface to enable siphon priming and fluid volume transfer between chambers.

2.2.3 Design of Analysis Device

The design of the centrifugal microfluidic disc driver (Figure 2) was created in SolidWorks. The driver is enclosed in a 12 x 8 x 7 inches box made of black acrylic sheets with

aluminum extrusions for the frame (Fig 2a). The box is called PPAS Cube for its shape and portability and is powered by a 12 V battery through a cigarette lighter interface. A car battery can power the Cube in areas with no reliable electricity. The system is controlled by a Raspberry Pi (CPU) with the New Out Of the Box Software. A 7-inch LCD touchscreen provides the graphical user interface (GUI) that enables users to start and stop the assay with a touch of button and to monitor the progression of the test. The subsystems (Fig 2a and described in detail below) inside the cube are driven by a program written in Python, which automates the speed and duration of the centrifugation, the control for the temperature feedback, the LED lights for image capture, camera function, the digital image processing, and the GUI. The prototype unit is less than 2 kilogram in weight (Fig 2b).

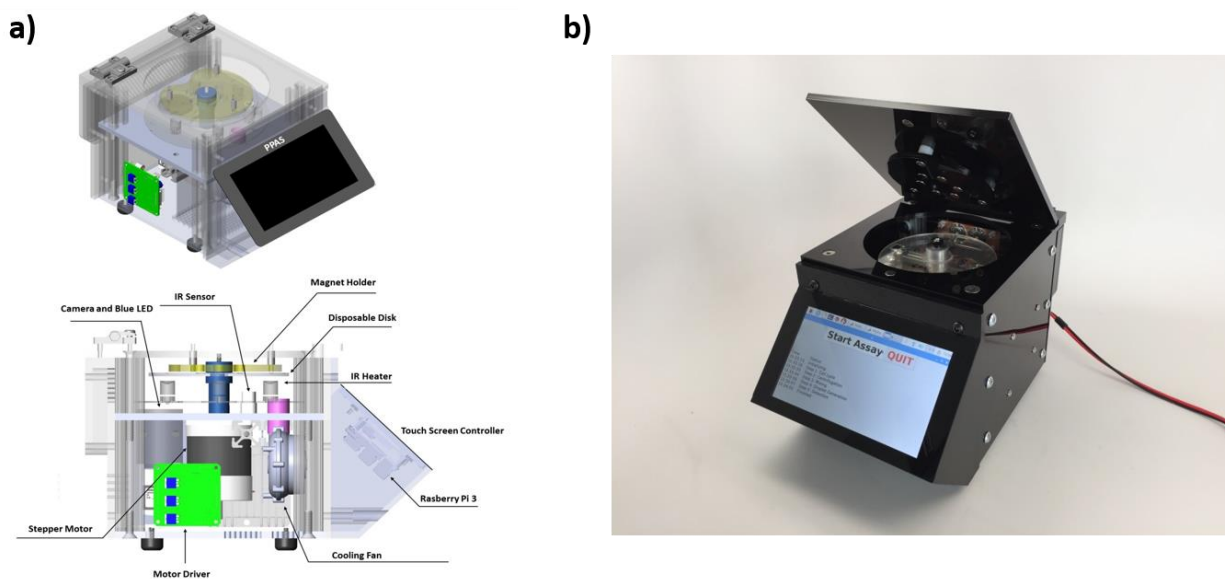


Figure 2. a) Solidworks illustration of assembled PPAS instrument with the bottom image highlighting the critical subcomponents and systems b) Actual prototype assembled and used for testing the disc.

Subsystems in the PPAS Cube are shown in Fig 2a. Mechanical subsystem drives the rotation of the disc. A motor controlled by a motor driver board is connected to the CPU via a

USB interface. An encoder on the motor shaft records the position of the motor and transmits the data to the motor driver. The motor and encoder are powered by 36 V and 5 V electricity, respectively. A permanent magnet holder positioned above the disc at the radial location of the sample lysis chamber moves the small metal disc together with the glass beads inside the chamber during disc rotation for cell lysis by bead-beating.

Thermal subsystem controls the desired temperature for LAMP reaction (65° C for *E. faecalis*). The amplification chamber is heated by one 5W Infrared (IR) lamps that are connected to the CPU via its own driver board. The IR lamp is located at same radial position below the reaction chamber and provides non-contact heating to the disc. An IR sensor is connected to the CPU via an Analog-to Digital Converter (ADC) and sits above the disc to provide feedback on temperature during amplification. The IR sensor is supplied by 5 V electric current via an analog signal between 0 and 3.3 V. Using an ADC, the digital signal is sent to a proportional-integral-derivative (PID) control feedback system to modify the duty cycle of the pulse width modulation driver and in turn, maintain the temperature at 65° C. The CPU outputs a 3.3 V pulse-width modulation (PWM) signal to modulate the brightness/heat of the lamps.

To demonstrate the proof-of-concept amplification, images of the amplified droplet array on – disc were captured using a traditional microscope and analyzed in ImageJ using a thresholding technique to discriminate between the positive and negative droplets. However, the optical subsystem integrated into the analysis instrument is designed for detecting target amplification using fluorescence signal. A 450nm LED excite the reaction chamber from the side of the disc to illuminate the fluorescent as well as total number of droplets, respectively. A camera located above the disc is used to capture images of the droplet arrays in the reaction chamber. The LEDs are controlled by on-and-off relays from the CPU, while the camera is

connected via a USB interface. Once the images are captured, they are analyzed using the Python API of OpenCV, a popular image processing tool. Filters are implemented to pre-process the image to optimize and automate detection for multiple images. A circle detection method (Hough circle transform) is used to first to detect the number of fluorescent (positive) droplets and then detect the total number of droplets. The number of blank (negative) droplets is computed by deducting the fluorescent count from the total count. The concentration of target pathogen in water is characterized by the following equation based on Poisson statistics ("Digital Droplet PCR Applications Guide", 2020):

$$Concentration = \frac{-\ln\left(\frac{N_{neg}}{N}\right)}{V_{droplet}}$$

Where,

Concentration= copies/volume

N_{neg} = number of negative droplets

N = total number of droplets

$V_{droplet}$ = volume of each droplet

In the future, the concentration can be reported on the PPAS interface, allowing the user to compare results to acceptable concentration values and determine the safety level of the sample.

2.3 Results and Discussion

2.3.1 Fluidic Integration of ddLAMP assay on-disc

In the basic workflow of the ddLAMP assay there are several key steps: 1) lysing the cells in the original sample through mechanical, chemical, thermal etc., means, 2) separating the

DNA from the cell debris and waste through centrifugation, elution, etc., 3) Metering a specified volume of the DNA sample and mixing it with the LAMP mastermix reagents, 4) Dividing the bulk reaction mixture into many microreactors or droplets, 5) adding droplets to a microcentrifuge tube and placing it in a thermocycler at 65°C for 30 minutes to initiate heating and amplification, and 6) quantifying the droplets post-amplification through image capture (e.g., flow cytometer, microscope) and image processing (e.g., ImageJ, custom image processing tools). Although this assay is shorter in comparison to culture methods, you have the use of several expensive equipment and material waste as well as the lag time in between steps for user handling.

Figure 3a shows how the benchtop ddLAMP assay was transferred onto the disc to mimic the same steps and eliminates user handling, material waste, and expensive equipment. The disc includes five functional units for cell lysis and DNA extraction, reagent holding, sample and reagent mixing, droplet generation, and amplification and detection. The integrated fluidic system on-disc is first tested using color dyed water to observe the flow pattern, volume control, mixing and metering (Fig 3b-g).

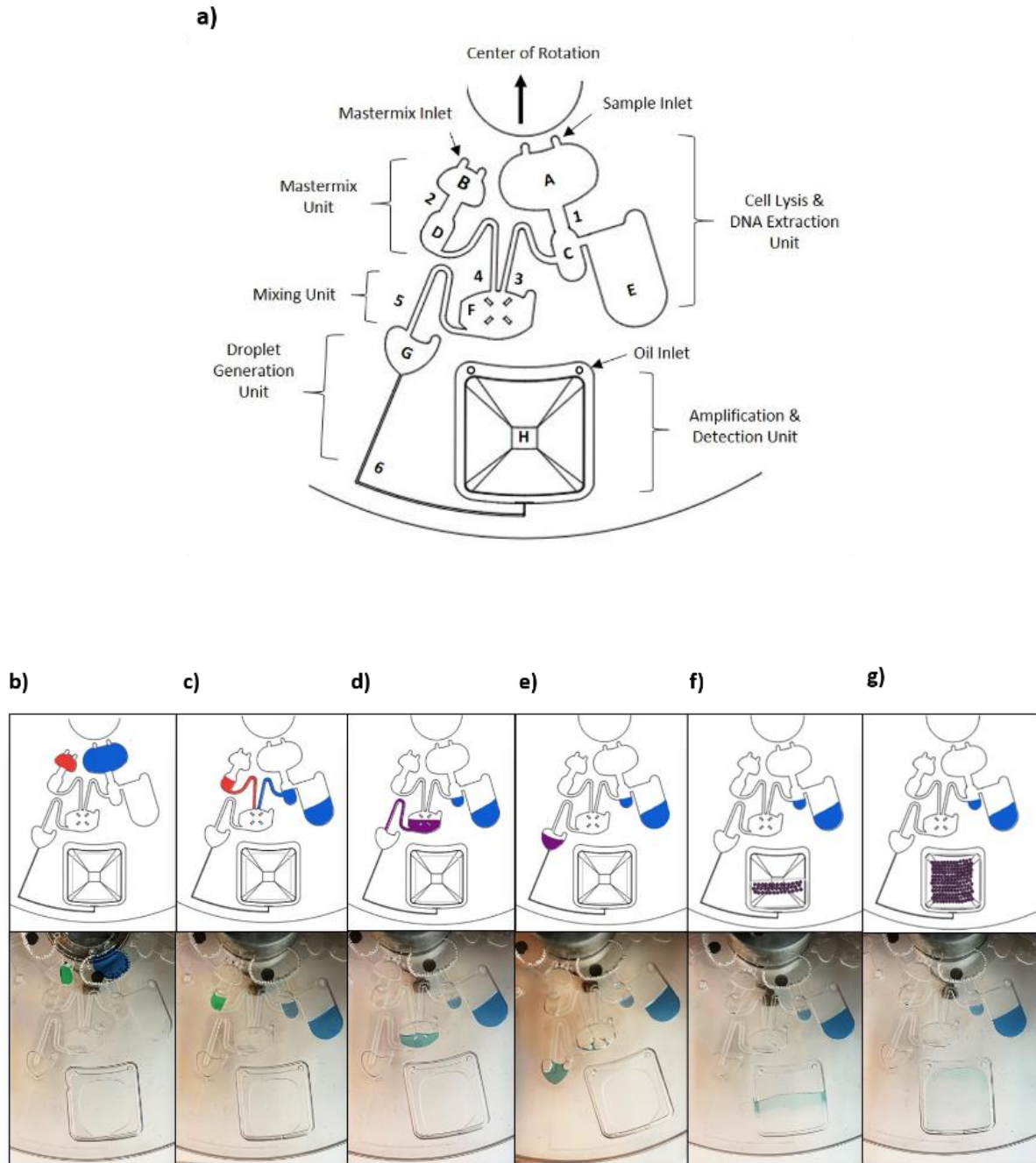


Figure 3. a) Schematic of disc design depicting main steps of ddLAMP assay. b) Cell lysis c) Centrifugation, DNA extraction/metering and siphon priming d) Mixing of mastermix and sample DNA and siphon priming e) Bulk reaction mix preparing for droplet generation f) Droplet generation g) Amplification and detection

Sample lysis chamber (A) with a sample injection inlet and a 3.35 mm diameter metal disc is filled with 0.1- 0.125 g of 500 μm diameter silica beads for cell lysis by bead-beating (Fig 3b). The chamber is designed to hold a sample volume of 100 μL . Mechanical cell lysis is simulated in the chamber by rotating at 200 RPM for 6 minutes. The low rotation speed enables the metal disc in the chamber to oscillate from one side to the other with the aid of permanent magnets placed above the disc. The silica beads provide additional friction to break open the cells. The Mastermix (LAMP reagents) unit mirrors the sample lysis unit at the same radial location but is designed to hold a smaller volume of 23 μL . The reagent mixture remains in the chamber B during the cell lysis step as shown in the real time image in Fig 3b. The speed does not exceed the burst frequency of the passive valves (point 1 and 2 in Fig 3a), allowing sample fluid to remain in the chamber during cell lysis. A more detailed view can be seen in in Figure 4.

Following cell lysis, an increase of the rotation speed to 2000 RPM for 20 seconds (Fig 3c) exceeds the burst frequency of passive valves at point 1 and 2, allowing the sample and reagents to flow into chambers C and D (Fig 3a), respectively. This design of the DNA extraction unit and speed change simulates centrifugation, extraction, and metering. As the sample flows into chamber C at a high speed, DNA supernatant is separated from cell debris and approximately 2 μL is metered for downstream amplification; excess sample is forced into the overflow waste chamber E (Fig 3a).

An brief pause (0 RPM) following the high-speed burst allows priming of the two hydrophilic siphons (point 3, 4 in Fig 3a) by capillary forces. Siphon channels are implemented in the design to allow metering of the DNA as well as to control the flow of sample and reagents to the next unit. The fluid halts at the interface to the mixing chamber F (Fig 3a) as shown in Figure 3c. A more detailed view can be seen in Figure 4.

The mixing of reagent and sample DNA in desired proportion is accomplished and shown in Figure 3d. The speed is increased to 500 RPM for 5 seconds to allow both the reagent and DNA to be released from the siphons into the mixing chamber simultaneously. The mixing chamber has four rectangular obstacles fabricated in an “X” shape to direct the fluid flow inside the chamber and act as a static mixer to cause turbulence and enhance mixing. Increasing the rotation speed to 2000 RPM for 20 seconds flushes the remaining fluid from the siphons. Due to the interplay between centrifugal and capillary forces, the quick high-speed change also prevents fluid from flowing through the subsequent siphon (point 3 in Fig 3a) prematurely. A more detailed view of this can be seen in Figure 5.

A second brief pause(0 RPM) in rotation following the mixing step allows priming of the hydrophilic siphon channel 3 (Fig 3d). The sample in the mixing chamber is then released through the siphon at 500 RPM for 30 seconds and enters an intermediate holding chamber G (Fig 3a) as the bulk amplification reaction mixture as shown in Figure 3e.

The final step of the fluid integration is to split the bulk reaction mixture into thousands of reaction-in-oil droplets (Fig 3f). This is achieved by pushing the bulk reaction mixture through a L-shape tapering channel (point 6 in Fig 3a) into the droplet generation chamber H (Fig 3a) that is prefilled with approximately 60-70 μL of HFE 7500 oil and fluorosurfactant mixture. Droplets are generated through a centrifugal step emulsification technique (Schuler et al., 2015) where the height and width of the channel exit (nozzle prior to chamber H) are most critical for the size of the reaction-in-oil droplet. As the disc spins, the reaction mixture is pushed through the channel and passes through the nozzle before it steps down into a wide and deep chamber that is filled with oil. Here, the sudden change in pressure at the nozzle due to this step and the surrounding oil helps to form the droplets. Variations in channel dimensions caused by CNC

fabrication and manual assembly of the disc, caused variations in droplet generation speeds and droplet sizes among the same disc and between different discs. However, in most instances, rotation speeds ≥ 1000 RPM for ≥ 90 seconds was sufficient to generate homogenous droplets. Additionally, since the reaction-in-oil droplets are lighter than the HFE 7500 oil, the droplets float above the oil layer as they are generated in the chamber (Fig 3f).

A pyramid-like structure is milled in the center of the chamber H and is surrounded by deep trenches (Fig 3a). When the speed of rotation is slowed below 60 RPM, the capillary force overcomes the centrifugal force and pulls the droplets toward the center of the disc. Additionally, the narrow gap between the top of pyramid and top polycarbonate layer allows the collection of reaction-in-oil droplets in a single layer (the dimensions are based on the expected diameter of one droplet) in the pyramid region (Fig 3g). Experimental results confirm previous studies (Schuler et al., 2016) that show the pyramid structure helps distribute of droplet in a single layer in the oil, minimizes droplet loss, and also serves to remove air bubbles due to air expansion during heating in the amplification reaction. At 45 RPM, the droplets remain in a single layer in chamber H and undergo isothermal amplification at 65°C for 30 minutes. The IR lamps are activated and are modulated by the IR sensor above the disc placed at the same radial position above the reaction chamber. Table 7 details the steps of the disc assay with the total approximate time of 45 minutes, eliminating much of the user-handling time and also minimizing material waste and use of expensive equipment.

Table 3. Step-by-step Protocol for ddLAMP Assay on-disc

Step	RPM	Time
Cell Lysis	200	6 min
Centrifugation and Extraction	2000	20 seconds
Siphon Priming	0	1 minute
Mixing	500, 2000	5 sec, 20 sec
Siphon Priming	0	1 minute
Holding	500	30 seconds
Droplet Generation	≥ 1000	≥ 90 seconds
Amplification	45	30 minutes
Detection	-	5 minutes
Total Time		~ 45 minutes

2.3.2 Effectiveness of On-disc Sample Preparation

To determine the cell lysis effectiveness on disc, a side-by-side comparison of on-disc assay with traditional bench top test-tube assay was carried in positive and negative *E. faecalis* spiked DI water samples. The cell lysis produced by the on-disc bead-beating method was taken out from the DNA supernatant chamber and used as the template for LAMP assay. The assay results were compared with the in-tube cell lysis assay where 0.1-0.125g of silica beads were added to a tube of 100 μ L sample and vortexed for 6 minutes, centrifuged at 10,000 RPM for 1 minute, and 2 μ L of DNA supernatant was extracted and added to the same 23 μ L LAMP mastermix. Both the on-disc and in-tube lysis method samples were amplified in a traditional thermocycler set-up. The negative samples showed no change in turbidity, while the positive LAMP reaction by both methods showed turbidity in the sample (Figure 4b shows results of on-

disc lysis with in-tube LAMP reaction). This result suggests the on-disc bead-beating method is adequate to extract DNA for on disc assay.

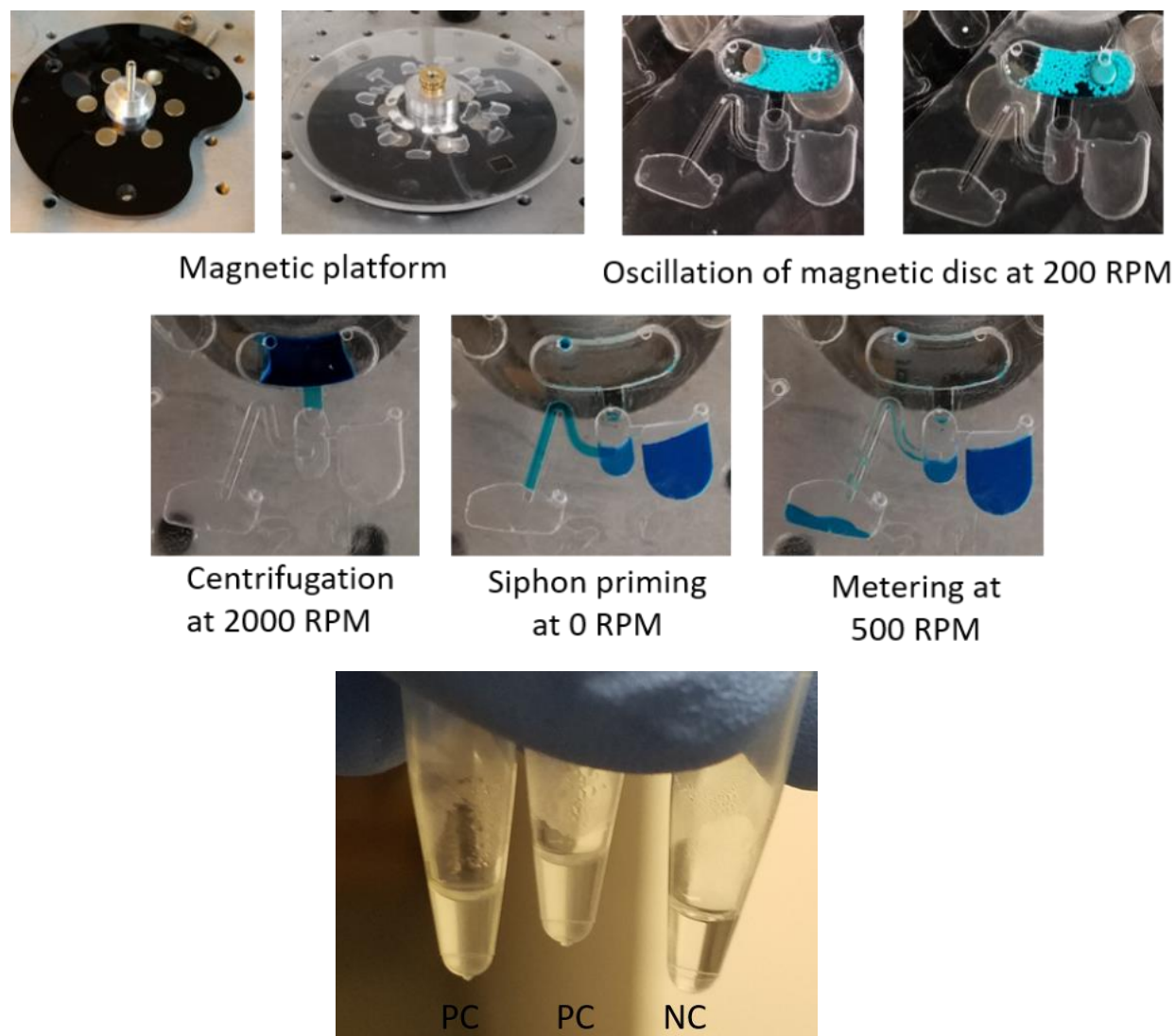


Figure 4. Top two rows of images shows schematic of basic fluidics of lysis, centrifugation, extraction, and metering on-disc. Third row shows metered sample extracted from on-disc for in-tube LAMP reaction confirmation (PC=positive control, NC=negative control)

Additionally, multiple experimental trials demonstrated that the integrated fluidic system could handle the reagent and sample mixing accurately. The bulk reaction collected from holding chamber G was again added to a tube and heated in a thermocycler for the amplification reaction.

The negative control with no DNA showed no change in turbidity while the positive controls showed turbid samples as illustrated in Figure 5.

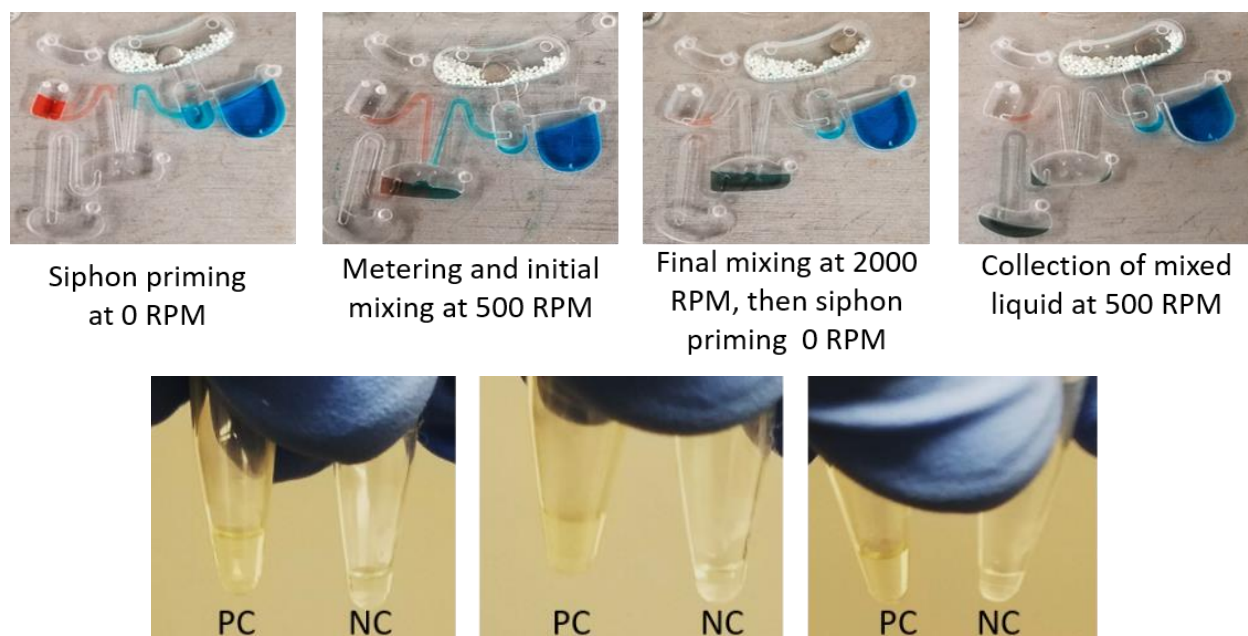


Figure 5 Top row shows schematic of basic fluidics of metering and mixing on-disc. Bottom row shows mixed sample extracted from on-disc for in-tube LAMP reaction confirmation

2.3.3 On-disc detection of *E. faecalis* in Spiked DI Water Samples

Successful amplification was achieved on-disc with serially diluted *E. faecalis* samples (10^4 - 10^6 CFU/mL) that were tested simultaneously due to the multiplexing capabilities of the disc design. Microscope images of different areas of the amplification chamber were captured to perform manual and automated image analysis and quantification (described in section 2.3.4). Figure 6a-d show representative images of each sample illustrating the proportional decrease of the positively amplified droplets with the dilution of the *E. faecalis* in the water samples. ddLAMP on-disc results are compared to traditional culture methods in Figure 6e. Similar to other molecular biology-based methods, the on disc amplification over estimates the target concentration than the culture-based methods likely due the presence of target DNA in the

damaged non-viable cells that is still detected in the LAMP assay. Additionally, variations and limitations with fabrication resolution of channel dimensions lead to limitations on droplet size and number which also have the potential to introduce bias and uncertainty into the calculations.

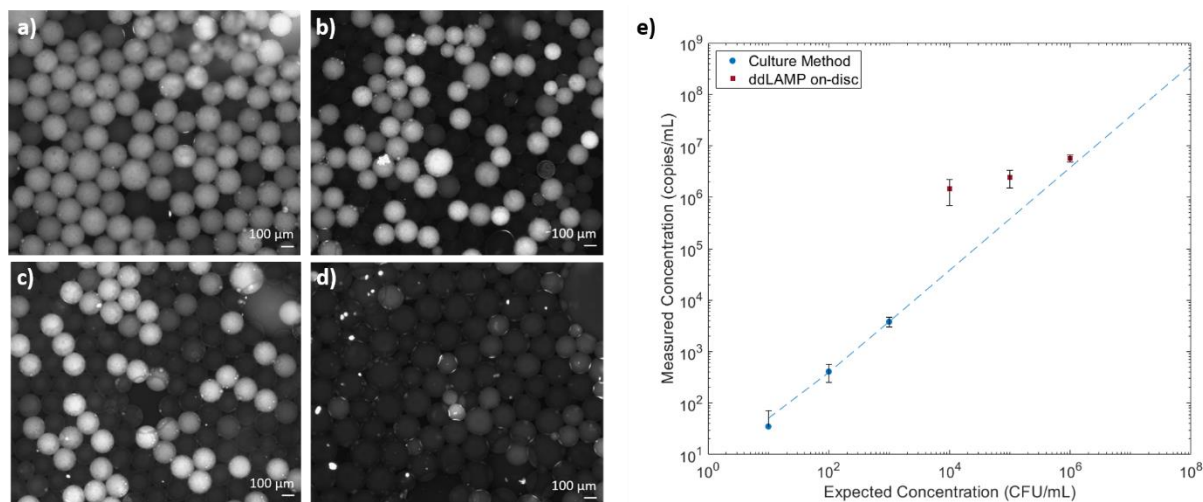


Figure 6. Representative microscope (5X magnification) images of droplets post-amplification. Positive (amplified) droplets are represented by the white or light grey color while the negative (non-amplified) droplets are represented by the black or dark grey colors. a) 10^6 CFU/mL (expected concentration) image b) 10^5 CFU/mL (expected concentration) image c) 10^4 CFU/mL (expected concentration) image d) Negative control (no DNA added) e) Plot of culture based results compared to ddLAMP results of the aforementioned samples

2.3.4 Image Processing and Quantification

Microscope images were captured and quantified using ImageJ and used to calculate the concentrations in Figure 6. In ImageJ, the negative control images were used to process the background signal and a thresholding technique based on pixel intensity was utilized on the serially diluted samples (Figure 6 a-c) to discriminate between the positive (white/light grey droplets) and the negative (black, background droplets). Based on the thresholding, ImageJ created the binary black and white images to enable easier discrimination. Droplets were then manually counted to assess the total positive and the total number of droplets in each image. To

utilize detection capabilities in the analysis instrument, an automated quantification method was also developed in Python and preliminarily tested with the aforementioned microscope images. Images processed with the automated method are shown in Figure 7. Concentration results from the image processing code are consistent with the calculations made in ImageJ. Ideally, concentration of target pathogen can be returned upon amplification without intermediate manual procedures. Although this demonstrates a step to further automate the system, there are several limitations and can be visualized in Figure 7. The images available to optimize the code was limited, and the code is not tested for extreme lighting conditions (though it is unlikely to happen inside the PPAS cube). As seen in Figure 7, irregular sized droplets (due to the droplet stability during the amplification reaction) may not be captured by the droplet detection program and ultimately will affect the droplet counts used to compute pathogen concentration. Additionally, if droplets generated are much smaller than the gap between the pyramid structure and the top of the chamber, multiple layers can form causing difficulty in detecting anything below the top layer. Despite these shortcomings, the results are comparable to the manual detection results, providing sufficient evidence to support the capabilities of our automated image processing scheme.

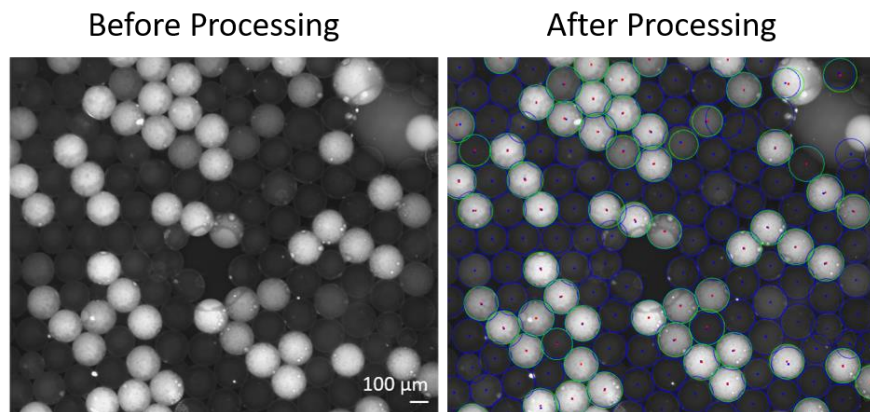


Figure 7. Automated image processing applied to ddLAMP results. Blue circles represent the total droplet count while the green circles represent those that are supposed to be the positive, or amplified droplets.

2.3.5 Challenges and Limitations

Two critical issues that affected successful amplification included generation of stable droplets and the precision of the temperature control in the amplification chamber. Although the reaction chamber was designed to help minimize air bubbles, pressure fluctuations due to the temperature led to merging, collapsing, or evaporation of the droplets in many experimental trials. Empirical experience and literature indicated that smaller sized ($\leq 100 \mu\text{m}$) droplets are more stable during heating and experience less coalescence (Figure 8). The droplet size is determined by the geometry of the channel at the chamber interface. Because the CNC is sensitive to vibrations in the surrounding environment and is more apt to machining dimensions greater than $100 \mu\text{m}$ with less variability, finer control and advanced machinery is necessary to consistently generate discs with sub- $100\mu\text{m}$ channel dimensions and droplet sizes. Due to these limitations, the channels we machined ($\sim 75 \mu\text{m}$ height and $\sim 120 \mu\text{m}$ width) produced variable droplet sizes between $150\text{-}200 \mu\text{m}$ but were still relatively stable during the heating process and demonstrated successful amplification. Other fabrication methods (laser cutting, 3D printing, and rapid prototype injection molding) were attempted, but many were limited to $>100 \mu\text{m}$ resolution and varying surface roughness which created additional variables. Moving to mass manufacturing practices such as injection molding can eliminate these fabrication variabilities

and provide a viable way to consistently machine smaller channels and thus produce smaller, more stable droplets.

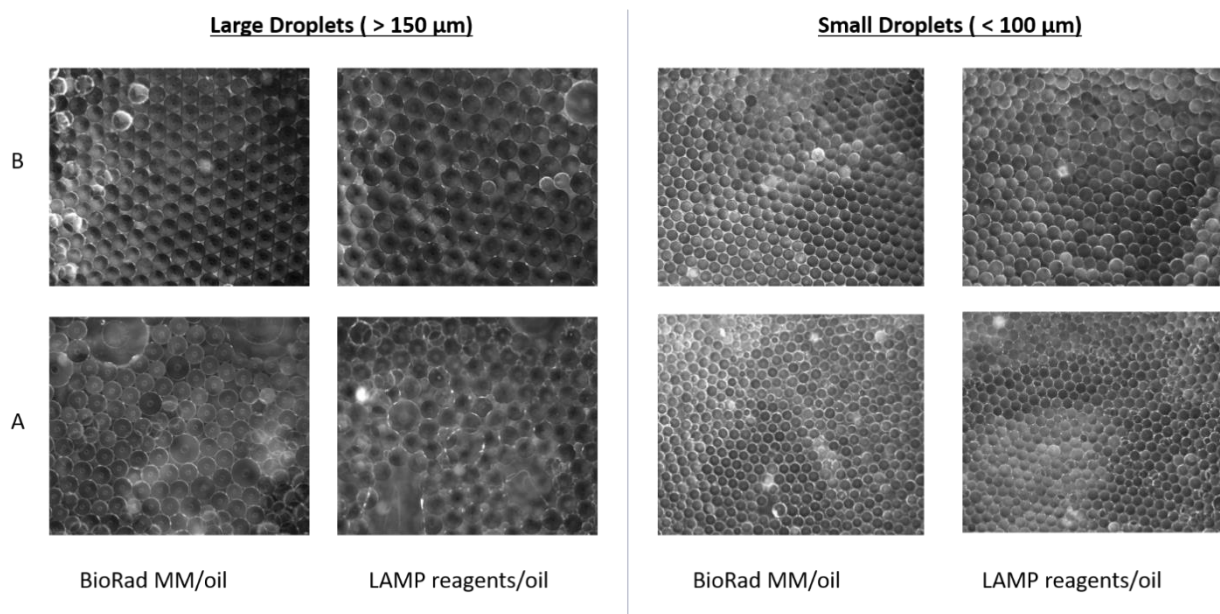


Figure 8. Representative microscope images of various droplet sizes before and after LAMP heating. B and A represent before heating and after heating, respectively. Commercial compatible oil/MM (BioRad) was compared to LAMP reagent used in this experiment. In both cases, bigger droplets appeared less stable overall after the heating step.

Additionally, the temperature feedback sampling rate, rotation speed, and PID parameters are critical in reaching the setpoint temperature quickly, minimizing overshoot and oscillation, and ultimately maintaining the setpoint temperature throughout. By testing with different IR sensor configurations (above or below disc), it was found that there was almost a 10°C difference between the top and bottom of the disc, calling into question how fast and how much heat was being delivered to the actual droplets in the chamber. Due to the material properties and thickness of the polycarbonate disc (~4mm) and varying thicknesses of features inside of the chamber, it appeared that there was a temperature gradient. This gradient was investigated by using an additional temperature feedback indicator. Temperature (specified at 65°C and 70°C) sensitive reversible liquid crystal adhesives (used to determine temperature of surfaces) was

placed on the pyramid surface inside the chamber; a specific color change indicated if it was above, below, or at the specified temperature. Comparing the temperature label with the IR sensor above the disc has helped to determine the actual temperature profile, the appropriate offset needed for the setpoint, how fast the disc reaches 65°C, and any fluctuations during the 30-minute period. Comparison of heating profile to the temperature label during one heating trial is shown in Figure 9. Additionally, a low rotation speed of 45 RPM during amplification enabled a balance between heating from the IR lamps below the disc and cooling from rotation to prevent overheating. The temperature graph showed the successful control of in chamber temperature between 65 and 68°C during amplification which is adequate for LAMP assays.

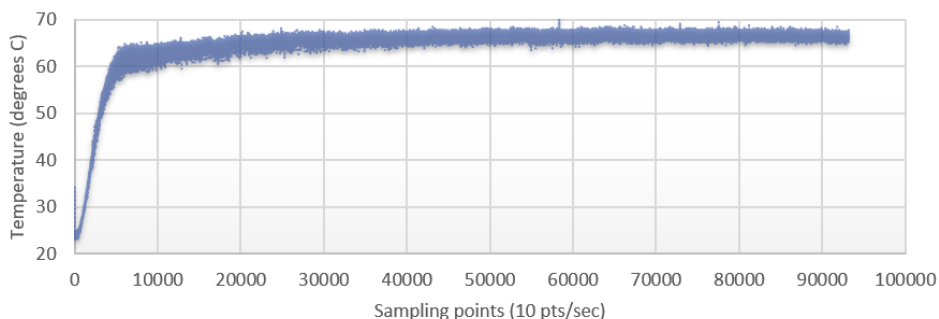


Figure 9. A) Temperature sensitive label inside amplification chamber. Green indicates that the label is at the specified temperature, blue indicates that it is above the specified temperature, and brown indicates that it is below the specified temperature B) temperature profile of top surface provided by IR sensor feedback at setpoint of $T=69^{\circ}\text{C}$ and PID parameters are $P=15$, $I=0.1$ $D=0$.

2.4 Conclusions

A prototype centrifugal microfluidic platform has been developed for the point-of-sample collection for detection of microbial contaminations in water. The operational unit and disc design are shown to be adequate in handling on disc cell lysis, reagent and sample metering and mixing, generation of reaction-in-oil droplets and on disc LAMP amplification of *E. faecalis*. The multiplex assay disc can complete multiple sample detection within 60 min with only

manual sample loading on-to the disc prior to the start of the assay. The reproducibility of the results is largely relied on the fabrication of the droplet generation and subsequent disc assembly. Minor variation in the dimensions of the droplet generation channel at the chamber interface can change the droplet size and number, and affect droplet stability during LAMP amplification. Transitioning the prototype to a large-scale manufacturer using injection modeling can potentially improve the reproducibility of the disc channels and quantification accuracy. Subsequently, adoption of the automated image quantification method and using the analysis device's image capture can streamline detection and quantification on-site. Furthermore, since this assay shows detection with spiked DI water samples, the next step is to utilize real-world water samples (e.g., wastewater, sewage etc.) to determine if the amplification or disc fluidics are affected by the presence of other contaminants or inhibitors. In the future, adopting a modular design of the disc (e.g. pie pieces fitting into a circle), could improve reproducibility as the fine control will only be necessary for fabricating a fraction of the disc at a time rather than the whole disc. The modular design can increase usability and multiplexing of samples.

CHAPTER 3

SAMPLE CONCENTRATION SYSTEM FOR WATER QUALITY ANALYSIS

3.1 Background

3.1.1 Common Methods of Sample Concentration in Pathogen Water Monitoring

In addition to the actual detection and enumeration of bacteria, sample collection and preparation are critical steps in the assay process. Environmental water samples range from those naturally occurring such as groundwater or surface water to water affected by human interaction (wastewater). The concentration of pathogens is much lower in environmental waters than clinical or food samples (where there usually is a heightened concentration of detected pathogen in a small volume) and thus require larger volumes to concentrate and assess relevant pathogen concentrations for human consumption. Water samples can undergo a variety of diluting processes such as wastewater treatment, and effluent flow into bigger bodies of water which consequently lead to a low level of target pathogen (Jofre and Blanch, 2010). Unlike clinical samples, environmental samples are further affected by the presence of various natural and unnatural materials some of which are known to inhibit enzyme activity for DNA amplification assays. For example, naturally occurring compounds include minerals such as bentonite, kaolinite, montmorillonite, divalent cations (Ca^{++} and Mg^{++}), or organic substances such as humic acids, fluvic acids, and tannins. Pollution and human interaction, however, include inorganics such as FeCl_3 and organics such as detergents, pesticides, hydro-carbons and pharmaceuticals (Jofre and Blanch, 2010). Thus, sample collection and preparation are critical steps in ensuring target pathogens can be effectively detected downstream.

Large volumes (>1 L) are collected and then undergo filtration on-site and/or processed at a centralized location off-site. Filtration, centrifugation, sedimentation, flocculation and coagulation are common pre-concentration methods (Bridle et al., 2015). Membrane filtration is an approved method of the EPA for step 1 in the process to detect *E.coli* and Enterococci ("Approved CWA Microbiological Test Methods | US EPA", 2020). Additional concentration methods such as centrifugation, filtration, immunomagnetic separation, dielectrophoresis, adsorption, precipitation, elution (Stevens, and Jaykus, 2004; Bridle et al., 2015; Xie et al., 2016). However, these benchtop processes require user expertise, expensive equipment, and time to reduce the volumes and enrich samples further increasing the “sample-to-answer” time.

3.1.2 Super Absorbent Polymer Beads for Water Sample Concentration

New emerging methods of bacterial concentration in environmental water sample utilize super absorbent polymer (SAP) beads (Xie et al., 2016; Wu et al., 2020). Super absorbent polymer beads are hydrogels containing a cross-linked structure that enables the beads to absorb water and expand up to 1000x the dry bead weight. Although SAPs have been around since the 1970s, much of their popularity has been due to their use in hygiene products, drug delivery systems, and agriculture (M.J.A.D. and Kabiri., 2008). Recently, Xie et al., used millimeter-sized SAPs to selectively concentrate pathogens (bacteria and viruses) in 10 mL environmental waters through selective absorption; by modifying the beads to have a negative surface charge and controlling the pore size, bacteria in the water are successfully repelled while the majority of the water is absorbed by the beads. Although Xie et al, was able to achieve a concentrated sample, several concentration steps were required to achieve an efficient bacterial recovery and reduced sample volume. Wu et al., aimed to improve this system by modifying the polymer chemical composition to enhance absorbency in different types of environmental waters, testing the

reusability of the beads, and incorporating the beads into a hand-pressed, 3D printed system capable of providing a portable platform. These improvements enabled a 10x volume reduction by one step while still achieving high bacterial efficiencies. However, this method still requires a number of “hands-on” steps for use in downstream detection, limiting its true incorporation into a field-testing arena with limited trained personnel.

3.1.3 Current Limitations and Proposed Method for Water Sample Concentration on Centrifugal Microfluidic System

In general, pathogen concentration methods have been limited in their implementation on the disc; thus far, only immunomagnetic separation has been used for the enrichment of pathogens (Cho et al., 2017; Strohmeier et al, 2013.). In these systems, only about ~100 μL of blood or cell lysate was used as the sample matrix. Unlike clinical samples, the challenge with respect to water samples is handling and concentrating larger volumes of water with a micro-scale volume system. As a result, sample preparation, and specifically concentration, have become the limiting factors preventing these platforms from really becoming a fully automated, portable system. The goal of this work is to determine how to concentrate milliliter volumes to microliter volumes on a centrifugal microfluidic system. More specifically, we aim to demonstrate the use of a simple 3D-printed component that integrates SAP beads for concentration and interfaces and distributes the concentrated water sample onto a centrifugal microfluidic disc, thus allowing hands-free concentration of a milliliter bacterial water sample.

3.2 Materials and Methods

3.2.1 Sample Concentration System Fabrication and Assembly

The microfluidic interface assembly is made up of three main layers: a hollow polylactic acid (PLA) cylindrical component (32mm x 37 mm) with space to hold sample and SAP beads, a transparent acrylic (3.175 mm thick) disc consisting of the chambers and channels for volume metering, and a top transparent adhesive layer (Flexmount) with vent holes (Figure 10). The designs were created in Solidworks with the hollow cylindrical component interfacing the acrylic disc with an outer diameter of 120 mm. The disc is 120mm in diameter with six identical 150uL chambers to hold the concentrated sample and a large waste chamber to catch any remaining liquid. The hollow cylindrical component is fabricated on a 3D printer (Raise3D N2 Plus) and will be called the Bacterial Concentration Unit (BCU). An epoxy (Pond Armor) was used to seal the inner and outer surface of the component to eliminate liquid absorption into the PLA. The acrylic disc was fabricated using a laser cutter. A sealant, seaming tape (Total Pond), was used to bond the cylindrical component to the acrylic disc and create a watertight seal. The outlet at the top of the BCU connects to an inlet on the bottom of the metering disc, allowing for seamless transfer of the concentrated sample onto the metering disc during rotation. The adhesive was aligned on top of the acrylic disc to seal the chambers and channels. Top screw #8-32 was used to thread set screw hole on BCU device and #8/32 x 1/2" set screw was used to safely secure the assembly to the motor spindle to allow it to rotate as one unit.

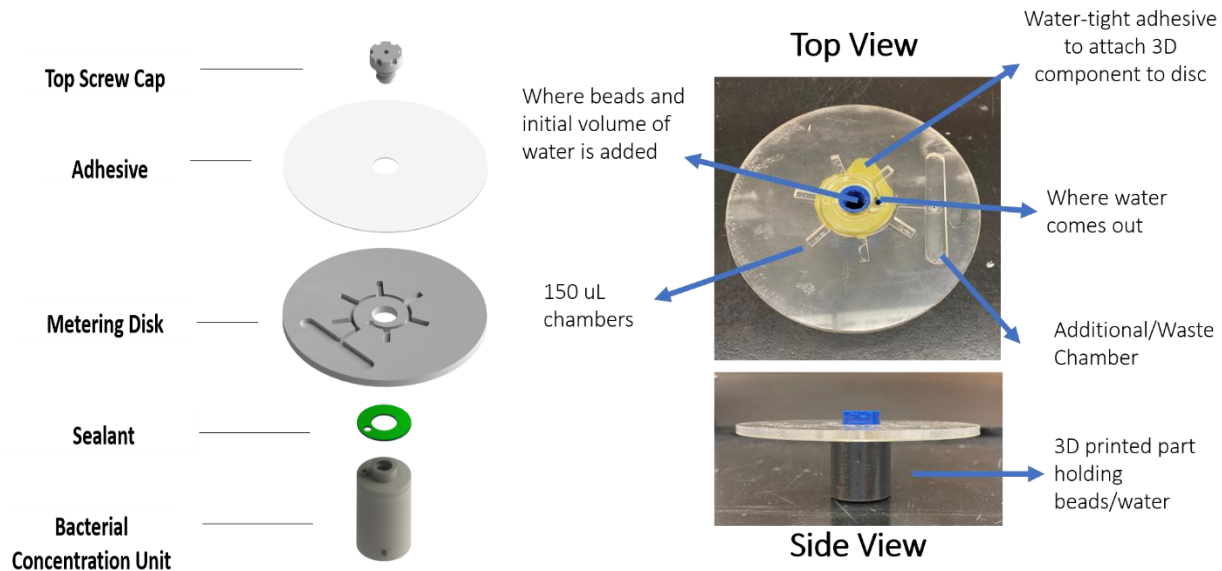


Figure 10. Left) Solidworks illustration of main layers of the sample concentration device. Right) Top view and side view of real assembled prototype

3.2.2 Bacterial Sample Preparation

To determine the bacterial concentration efficiency *E.coli* K12(ATCC 10798), another water quality fecal contamination indicator. *E.coli* was grown in LB broth at 37°C overnight. The culture was serially diluted in DI water and plated on LB agar plates to count colonies to determine the initial concentrations. Bacterial concentrations between 10^3 - 10^5 CFU/mL were then used for both stationary and on-disc concentration experiments. Following concentration, recovered samples were plated on LB agar plates to count colonies and determine recovery efficiency. Super absorbent polymer beads ranging from small (~100-500 μm diameter) to medium (500 – 900 μm diameter) in size were fabricated by the Hoffman group at the California Institute of Technology using previously described methods (Wu et al., 2020).

3.3 Results and Discussion

3.3.1 Integration of SAP Beads onto Centrifugal Microfluidic Platform

Figure 11 shows the design and basic strategy of the sample concentration device. The hollow cylindrical component is designed to fit securely on top of the motor to enable the whole assembly to rotate as one monolithic unit. The outlet at the top of the WTC connects to an inlet on the bottom of the metering disc, allowing for seamless transfer of the concentrated sample onto the metering disc during rotation. The metering disc is designed with six identical chambers that are sequentially filled as the sample is transferred onto the disc. As a proof of concept, 4 mL of *E.coli* spiked DI water was used demonstrate the concentration capabilities. Initially, SAP beads are preloaded into the hollow cylindrical component; then 4 mL water sample is pipetted in as. The SAP beads begin swelling from water absorption resulting in sample concentration. Once the SAP beads have swelled to capacity (time is based on size of the bead and absorption capabilities), the disc assembly is spun drive the concentrated sample up the sides of the walls and through the cylindrical component outlet. Through experimental trials, the critical RPM needed to transfer the liquid to the disc was 3000 RPM. Spinning at speeds ≥ 3000 RPM for at

least 1 minute enables the transference of the concentrated sample onto the disc, where it fills up the metering chambers sequentially in a counterclockwise manner.

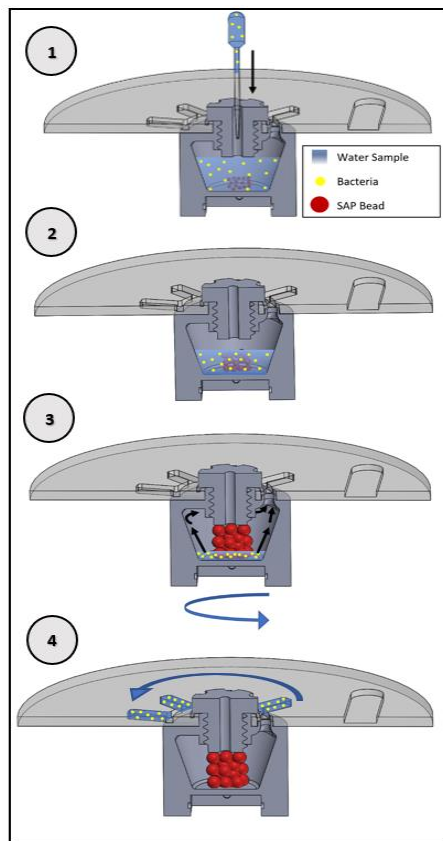


Figure 11. Schematic of sample concentration and transfer process using the sample concentration system. 1) Pipette sample into BCU component with preloaded SAP beads 2) Allow SAP beads to absorb water 3) Rotation at 3000 RPM to release concentrated sample from the BCU component 4) Concentrated sample is transferred successfully onto the metering disc

3.3.2 On-disc concentration of *E.coli* in Spiked DI Water Samples

Experiments integrating SAPs beads on-disc were initially compared with the stationary method where sample was added to a small beaker prefilled with SAP beads and allowed to absorb; concentrated samples were then manually recovered using a pipette. All DI water samples used were spiked with *E.coli* at concentrations between 10^3 - 10^5 CFU/mL to observe

concentration capabilities and bacterial recovery at various concentrations. Volume recovered and bacterial concentration were analyzed using two main parameters:

$$\text{Concentration Factor} = \frac{\text{Initial Volume}}{\text{Final Volume}}$$

$$\text{Recovery Efficiency (\%)} = \left(\frac{\text{Final Concentration} \times \text{Final Volume}}{\text{Initial Concentration} \times \text{Initial Volume}} \right) \times 100$$

Figure 12 shows the concentration factor and recovery efficiency of experiments with both the stationary and on-disc (rotation) recovery methods across different concentrations. Parameters such as bead size (medium size), bead amount (0.25g), initial volume (4 mL) and absorption time (13 minutes) remained the same in both sets of experiments. Across all concentrations, the sample volumes were reduced from 4 mL to an average of $269 \pm 38 \mu\text{L}$ in the stationary method and $604 \pm 61 \mu\text{L}$ in the rotation method. On average, slightly more than 2x more volume was recovered with the on-disc experiments than with the stationary method, most likely due to the centrifugal forces at play during rotation. As a result, the bacterial recovery efficiency across all concentrations in the stationary method was an average $18.38 \pm 4.93 \%$ compared to $48.23 \pm 10.05 \%$ of on-disc appeared. Again, we see slightly more than 2x more bacteria recovered in the rotation method than the stationary method across different concentrations. Since more volume is recovered on disc, more bacteria was also captured in this

volume. This demonstrates that the SAP beads can be effectively integrated on-disc and used for concentration without negatively impacting bacterial recovery.

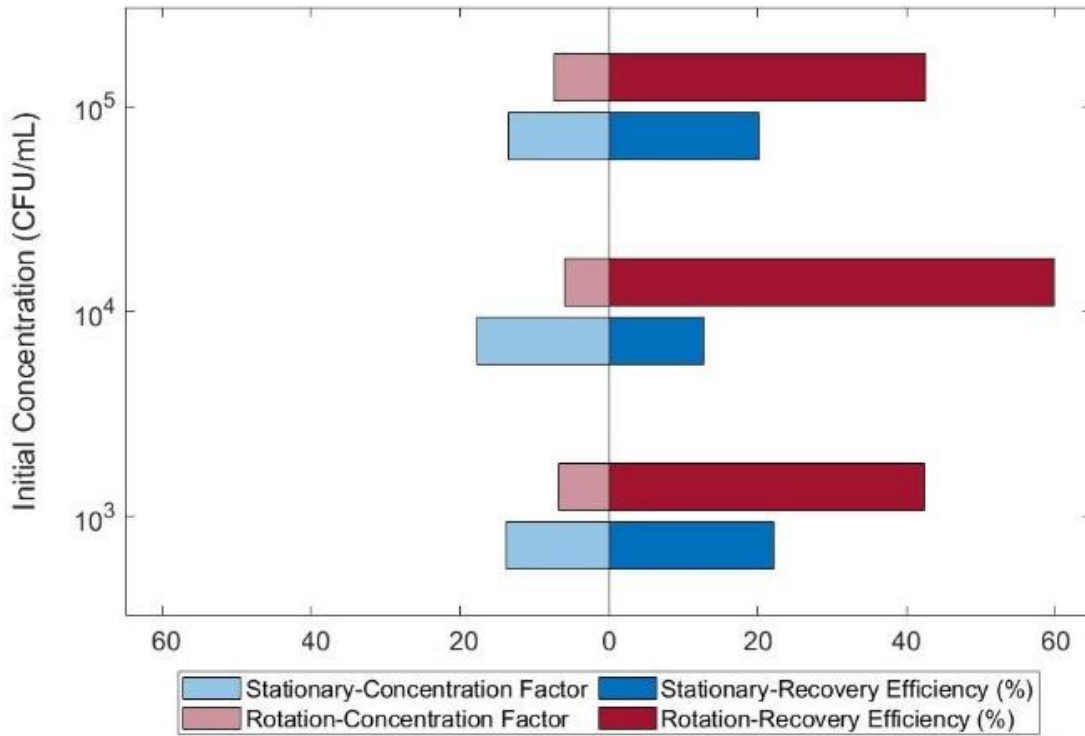


Figure 12. Concentration factor and bacterial recovery comparison between stationary (blue) and rotation/on-disc (red) experiments

3.3.3 On-disc concentration of *E.coli* in Spiked DI Water Samples using Different SAP Bead Sizes

Different bead sizes with varying absorption properties were also integrated into the on-disc assembly to assess the compatibility with the BCU component design. As previously mentioned in section 3.2, medium and small were fabricated and used for comparison in these sets of experiments. Parameters for each bead size were determined from preliminary experiments to reach a 5- 10X volume reduction for downstream bacterial recovery comparison. More specifically, for the small beads, 0.13g of beads were allowed to absorb for 5 minutes

while for the medium beads, 0.25 g were allowed to absorb for 13 minutes. In all experiments, the sample concentration device was loaded with 4 mL of DI water spiked *E.coli* (10^3 - 10^5 CFU/mL) and the device was spun at 3000 RPM for 1 minute.

Figure 13 shows the results of the experiments. While the concentration factors were similar based on the experimental parameters, the bacterial recovery efficiency of the small beads on average was 35.30 ± 5.90 % compared to the medium beads which had an average of 48.23 ± 10.05 %. The differences in bacterial recovery efficiencies can most likely be explained to the inherent differences in the absorption capabilities of the beads based on their size. Xu et al. explained that with while with smaller SAP beads you have a larger surface area and a higher absorption rate, this may lead to the adsorption of target species onto the beads, thus potentially decreasing the bacterial recovery efficiency. As the results show the similar trends with the literature, SAP beads of different sizes are compatible with the sample concentration device without negatively affecting the bacterial recovery efficiency.

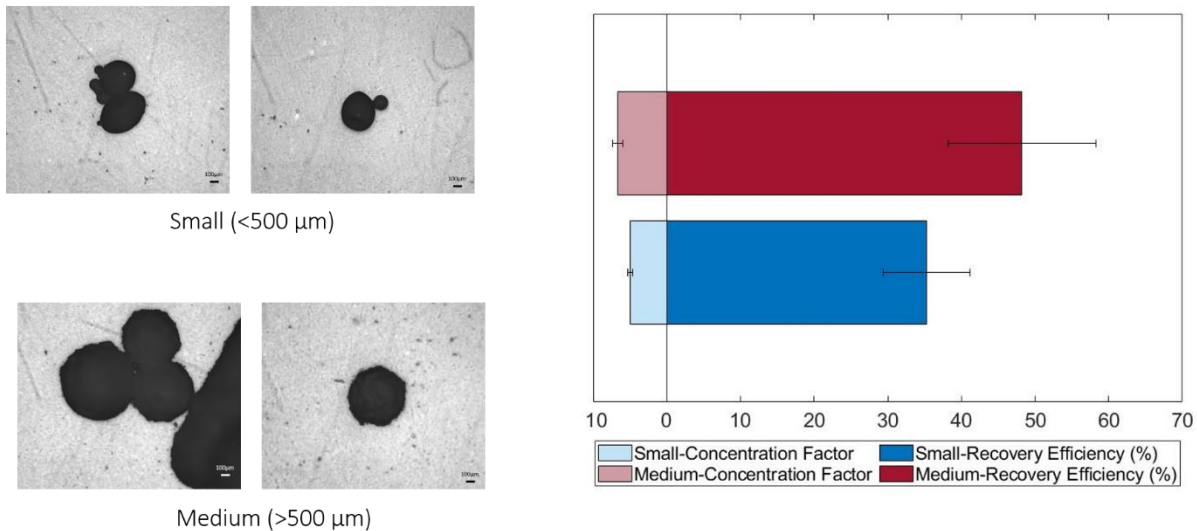


Figure 13. Left) microscope images of bead two different groups of beads used for integration onto WTC assembly. Right) Concentration factor and bacterial recovery for on-disc concentration using small beads (blue) and medium beads (red).

3.3.4 On-disc concentration of E.coli in Spiked DI Water Samples using Different Rotation Speeds

Finally, rotation speed of the sample concentration device was varied in combination with use of small SAP beads to see if concentration factor and recovery efficiency could be further optimized. In this set of experiments, 0.16g of the small beads were allowed to absorb for 5 minutes in 4 mL of DI water spiked with *E.coli* (10^3 - 10^5 CFU/mL). After absorption, the sample concentration device was spun at 3000 or 6000 RPM for 1 minute. Figure 14 highlights the results of these experiments. At 3000 RPM, an average of 720 ± 136 μ L was recovered across all concentrations while at 6000 RPM, an average of 879 ± 118 μ L was recovered. Due to the higher centrifugal forces present, spinning at 6000 RPM consistently recovered a slightly more volume than at 3000 RPM. While the over 100% recovery efficiencies can be attributed to small measurement errors in quantifying *E.coli* concentrations, we observe high recovery efficiencies at both speeds and across all concentrations most likely due to a combination of the modified bead amount used and rotation speeds enabling a higher volume recovery than would have been recovered using the stationary method. This study prompts the further investigation of how to optimize bacterial recovery through bead size, amount, absorption time, and rotation speed.

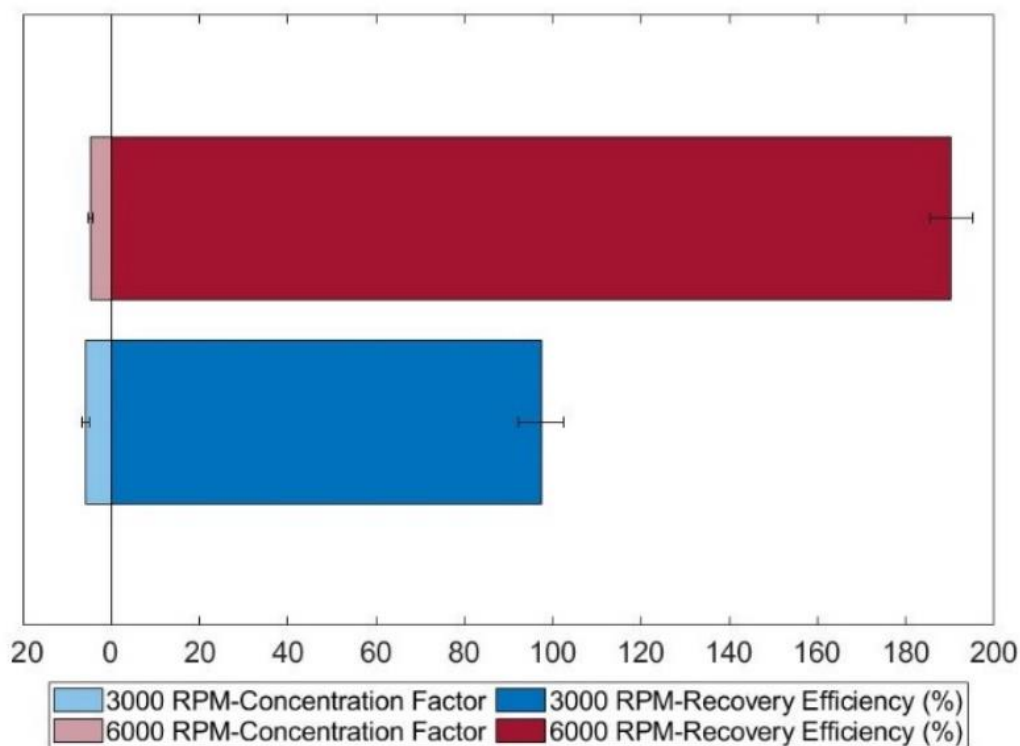


Figure 14. Concentration factor and bacterial recovery for on-disc concentration when recovered sample is transferred onto the disc at 3000 RPM (blue) and 6000 RPM (red).

3.4 Conclusions

The integration of SAPs beads onto a centrifugal microfluidic-based sample device for microbial pathogen concentration has been demonstrated. The device can accommodate milliliter volumes, enable concentration and volume reduction, and transfer the recovered microliter volume onto a disc without use handling. Additionally, the time and sample loss due to user-handling post-concentration is eliminated as the transference of recovered liquid onto the disc is seamless and can executed within 1 minute. A detection scheme and design can be easily implemented downstream of the collected concentrated sample on the same disc. With optimization of the dimensions of the BCU to hold larger volumes, the simple design of the device, user-friendly protocol, time reduction, minimization of sample loss, and easy integration

with downstream detection, make it highly viable for use at the point-of-sample collection.

Furthermore, we observe that rotation enables larger volumes to be recovered without negatively impacting bacterial recovery. Parameters such as bead size, amount, absorption time and rotation speed can be optimized in unique combinations to potentially improve the bacterial recovery. In the future, the device will be tested with real-world water samples to determine the effects of other contaminants on the concentration and fluidics of the device.

CHAPTER 4

ASSAY DEVELOPMENT FOR ASSESSING PATHOGEN VIABILITY AND INFECTIVITY IN WATER

4.1 Background

4.1.1. Common Methods of Assessing Viable Pathogens in Water Samples

In the environmental realm, traditional culture methods provide information about culturable, viable bacteria and remain the gold standard for understanding the bacterial infectivity and diversity ("Approved CWA Microbiological Test Methods | US EPA", 2020). However, the limitations here include not being able to capture non-culturable pathogens as well as the slow assay time compared to molecular methods (Jofre and Blanch, 2010; Váradi et al., 2017; Baymiev et al., 2020).

When PCR was developed in the late 1980s, researchers were then able to detect both live and dead bacteria as well as those that were culturable and non-culturable. Although this captured a wider variety of bacteria, differentiating between live or dead still remained a challenge. As shown in the previous chapters, bacterial detection in environmental samples is a complex, multi-step process. While we have discussed the use of DNA and how to incorporate both upstream and downstream aspects of DNA-based detection assay onto a microfluidic platform, a key limitation of some DNA-based platforms is their inability to distinguish between viable (live or active) and dead (inactive) cells that can lead to an overestimation of the proportion of infectious pathogens in a sample. This distinction is necessary for monitoring bacterial pathogens as well as assessing and managing the potential risk of infection and spread (Jofre and Blanch, 2010; Váradi et al., 2017; Baymiev et al., 2020).

4.1.2 RNA as a Marker for Assessing Viable Pathogens

In the 1990s, RT-PCR along with other RNA-based techniques were developed. Ribosomal RNA (rRNA) has been known to be a good indicator of potential metabolic activity due to its relatively short half-life and its increase in concentration during specific phases of cell growth (Halford et al., 2013; Bowsher et al., 2019; Baymiev et al., 2020). In addition, the natural abundance of rRNA as compared to DNA within cells, makes it a great target for detection without the need for target amplification (Halford et al., 2013). 16S rRNA in particular, is comprised of conserved and variable regions, allowing construction of universal primers and targeting of species-specific hypervariable regions (James, 2010). However, a major difficulty has been optimizing the use of RNA for direct detection without the need for target amplification methods like RT-PCR. Researchers are still met with challenges including complexity of design, high susceptibility to contamination, and potentially poor primer annealing resulting in nonspecific amplification leading to biased results (Bleve et al., 2003; Stadhouders et al., 2010). Consequently, there is a viable argument for exploring and expanding amplification methods beyond such techniques to improve specificity while maintaining the strengths of RT-PCR.

4.1.3 Signal Amplification and Enzyme-Assisted Target Recycling

Limitations of traditional nucleic acid-based target amplification techniques mentioned above have led to the development of unique signal amplification methods known as enzyme-assisted target recycling (EATR). Enzyme-mediated target recycling (EATR) is a linear amplification strategy that utilizes a nuclease-mediated cleavage of a reporter probe-target complex (Figure 15) . This technique of signal amplification for nucleic acid detection uses a wide array of target analytes ranging from mRNA to DNA. Most assays only require isothermal conditions and are less prone to nonspecific amplification and contamination. Several examples

of nucleases used in this amplification strategy include restriction endonucleases, Nicking endonucleases, Exonuclease III, Lambda exonuclease, Rnase H and Rnase HII, AP endonuclease, DNase I and Duplex-specific nuclease. With greater characterization of these emerging classes of nucleases, EATR has become a popular method due to the flexibility of the technique with a variety of probe types and reporters, simplified assay conditions, high specificity and the ease of incorporation into common multiplexing designs (Gerasimova and Kolpashchikov et al., 2014).

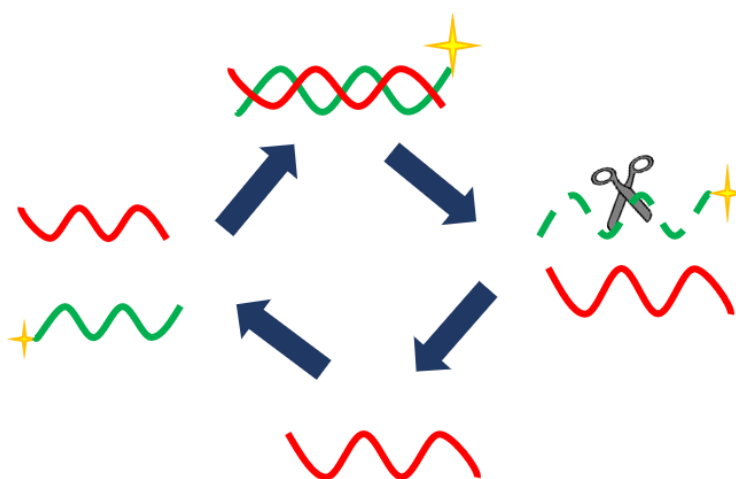


Figure 15. A basic enzyme mediated target recycling signal amplification scheme. Left) Target probe (red) hybridizes with tagged (yellow star) capture probe (green) Top) An enzyme with cleaving activity towards the capture probe is added and cleaves the capture probe in the duplex. Right) Following cleaving, the target probe is released back into solution. Bottom) Unbound target probe hybridizes with another uncleaved tagged capture probe. Labels released by enzyme cleavage can be collected for downstream detection.

4.1.4 Duplex-Specific Nuclease

Duplex-Specific Nuclease (DSN), a unique class of nonspecific duplex-cleaving nucleases originating from the *Paralithodes camtschaticus*, has been used for RNA signal amplification using an EATR scheme due to its sequence-independent DNA cleaving activity and inactivity toward RNA. Additionally, DSN displays preferential activity toward DNA in duplexes while exhibiting compromised cleaving activity in the presence of single mismatches within a 15 base-

pair range, enabling high probe specificity (Shagin et al., 2002). This property of DSN has spurred recent investigation into the nuclease's potential for signal amplification in miRNA-based cancer diagnostics. In the very basic strategy (seen in Figure 16), a RNA (target) is introduced into a solution with a complementary ssDNA modified with a reporter (e.g., fluorophore) and allowed to hybridize to form a DNA-RNA duplex. DSN is then introduced and cleaves the ssDNA in the duplex, releasing both the reporter and intact RNA target back into solution. Thus, the target RNA can be recycled and hybridized with remaining uncleaved ssDNA reporter probes. As this cycle repeats, more reporters are accumulated in solution and are collected for downstream detection via different detection methods ranging from optical to electrochemical (Qiu et al., 2015)

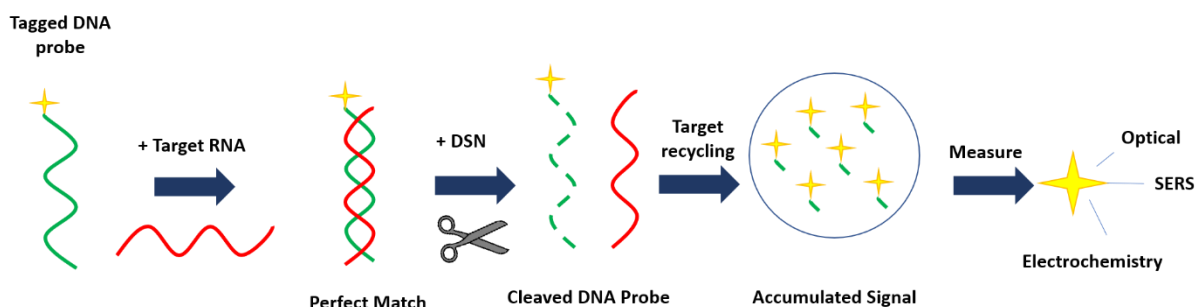


Figure 16. DSN-mediated Signal Amplification Scheme

4.1.5 DSN-mediated Strategy for Specific Bacterial Detection

Common uses for DSN in the biomedical field have been for use in construction of cDNA libraries, single-polymorphism detection, RNA sequencing, telomeric overhang detection, and most notably microRNA detection (Gerasimova and Kolpashchikov et al., 2014.). The EATR strategy utilizing DSN offers potential in detection of ribosomal RNA (rRNA), and specifically 16S rRNA for bacterial identification and detection. By targeting distinct regions of the bacterial genome, researchers have been able to distinguish between closely related species. However, with the presence of many similar regions both between different species as well as

within the 16S genome itself, it becomes increasingly important to accurately identify the sequence of interest. When using short probes to target these sequences, it is extremely probable that there will be a degree of mismatched hybridized pairs, potentially resulting in incorrect identification of pathogens (Janda and Abbott, 2007). DSN has the potential to be utilized in these situations due to the ability to discriminate between perfectly hybridized and mismatched pairs, resulting in the absence of both probe cleavage and signal amplification in the presence of mismatched duplexes (Figure 17). DSN has been previously demonstrated using miRNA as a target for cancer diagnostics due to its short sequence size, naturally low concentrations, and close homology of different miRNA sequences (Huang et al., 2019). Furthermore, applications for multiplexing have been well explored for simultaneous detection of different miRNA sequences in clinical samples (Wang et al., 2018; Xu et al., 2016).

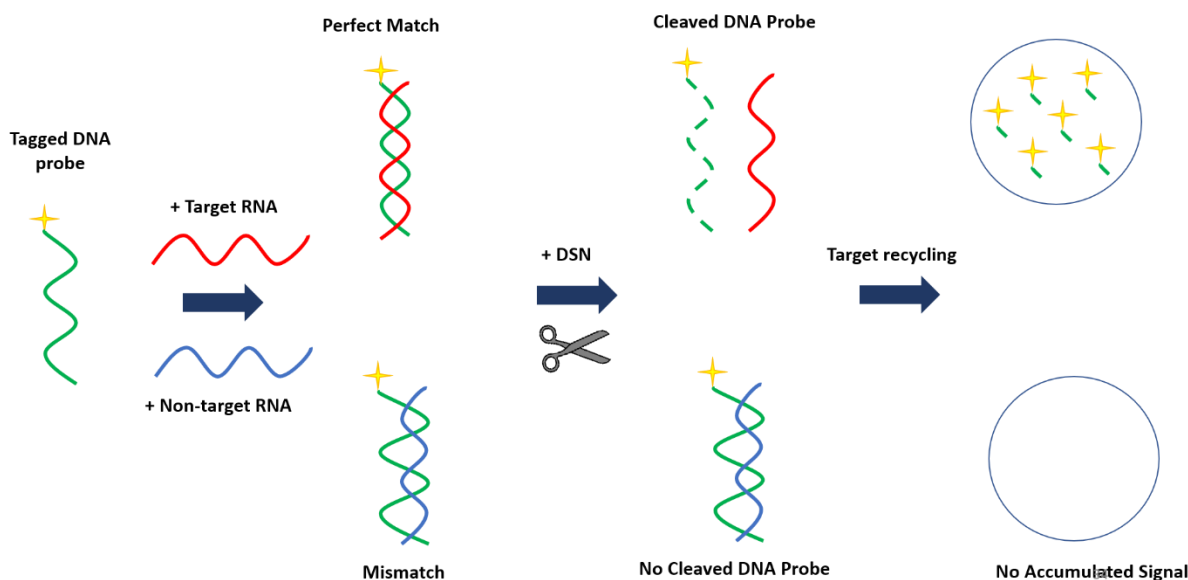


Figure 17. DSN-mediated signal amplification scheme highlighting the effect of perfect matches versus mismatches in solution.

DSN-mediated signal amplification has not been extensively investigated for bacterial rRNA. Accessibility of rRNA regions and design of rRNA probes were difficult in the past due to limited technology and could be cited as reasons why DSN had not been initially used in

bacterial genomics. As opposed to miRNA which is typically short 15-25 bp regions in low abundance, ribosomal RNA are longer 1600 bp regions in higher concentrations. Due to the size of rRNA, there are significant secondary structures that have made it challenging to characterize probes with high binding efficiency to certain regions of the RNA (Frickmann et al., 2017). However, with improvements in sequencing, databases for species-specific probe construction and published performance of similar probes in real cell sample analysis, DSN has the potential to be an ideal candidate for use in bacterial diagnostics (Medlin et al., 1988).

4.1.6 DSN-mediated Strategy for Viable Bacterial Detection

While RNA displays great promise for bacterial detection because of characteristics highlighted above, another major asset is its ability to help distinguish between live and dead bacteria, a necessity for environmental testing for understanding transmission of disease and assessing risk. This feature is attractive for ribosomal RNA detection due to rRNA multiplication correlated with cell growth, enabling a form of exponential amplification of the target during the growth phase as well as an initial indication of the state of the pathogen (Halford et al., 2013; Bowsher et al., 2019; Baymiev et al., 2020). By monitoring the growth of bacteria over a shortened exponential growth phase, researchers have been able to predict the increase of rRNA concentrations in active cells and determine the infectious capabilities of the sample (Figure 18). By incorporating this short-term culture technique with the aforementioned DSN – mediated strategies, we can discover information about the quantity of viable, infectious pathogens in the sample and use the information to assess the public health risk.

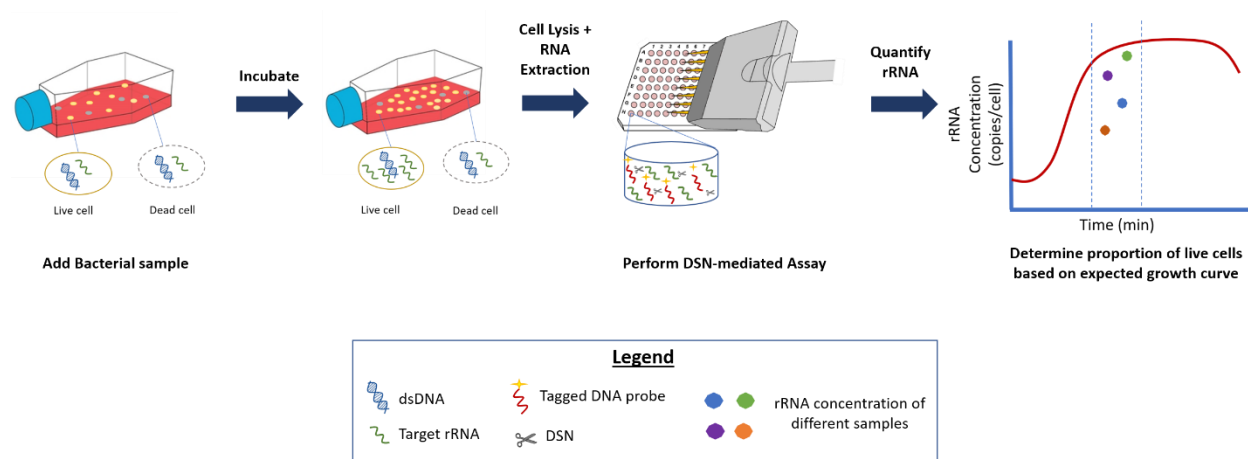


Figure 18. Potential integration of DSN-mediated assay with upstream incubation step to assess viable pathogens in a sample.

4.1.7 DSN-mediated Strategy Detection Platform Versatility

Despite being a highly specific strategy with respect to RNA targets, the DSN-mediated technique can be easily incorporated onto a multitude of different detection platforms ranging from optical and electrochemical detection to mass spectrometry and SERS and has been demonstrated in miRNA targeted approaches due to the adaptability of the signal amplification format (Peng et al., 2018; Wang et al., 2015; Li et al., 2016 ; Liu et al., 2015 ; Shi et al., 2018; Wu et al., 2018). Additionally, DSN-mediated signal amplification has been successfully employed in conjunction with a wide range of other amplification schemes (including HCR, enzymatic, RCA) to reach extremely low concentration levels, highlighting its flexibility in existing miRNA detection schemes while improving the limit of detection (Ying et al., 2017; Kim et al., 2016; Zhang et al., 2019). For example, the versatility of the technique can be seen through the incorporation of DSN into successful miRNA detection schemes of let-7d in vastly differing platforms with varying labels and secondary methods of target amplification (Xu et al., 2018; Tao et al., 2017; Lu et al., 2017; Zhang et al., 2016). This platform flexibility enables potential seamless integration of detection of other similar targets such as bacterial rRNA.

For these aforementioned reasons, developing an assay based on a DSN-mediated target recycling scheme to achieve rRNA signal amplification for targeting pathogens in water will be explored in this chapter. Due to the need for assessing bacterial viability, diversity, and quantification, water samples would be an ideal sample matrix to demonstrate this strategy.

4.2 Materials and Methods

4.2.1 Bacterial Sequence Probe Design

16S rRNA is a 1600 BP sequence found in almost all bacteria and highly conserved, making it a useful target for bacterial detection. Within the 1600 BP, there are conserved regions, those that are consistent within the taxonomy and useful for things like universal PCR primer design, and variable regions, those that have a species-specific signature sequence to help distinguish bacteria and useful for things like species-specific primer design. There are 9 variable regions within 16S rRNA, however the V3 region contains the greatest number of single nucleotide polymorphisms or differences between bacteria and has been widely used as a target marker in the literature, making it an suitable target region for exploring E.coli detection. Subsequently, specific sections within the V3 region were identified as target regions based on previous work indicating rRNA probe accessibility (ability of a capture probe to hybridize with the target rRNA sequence based on the structure and thermodynamics of the 16S rRNA molecule) (Yilmaz and Noguera, 2006).

Two different unique sequences from the *E.coli* 16S rRNA V3 region were identified and tested *for* feasibility with the DSN-mediated assay (Table 4). 447-467 BP was chosen and the uniqueness of the sequence to E.coli was also validated using the Basic Local Alignment Search Tool (BLAST) and found that there were only similarities with *Shigella (boydii, sonnei, flexneri,*

dysenteriae) and *Brenneria (alni)*. Synthetic ssDNA capture probes and RNA target probes sequences are shown below and produced by IDT. The other sequence, 467-486 BP was highlighted in Yilmaz et al., for its rRNA accessibility. Additionally, both were fluorescently labeled with a tag on the 5' end to produce a fluorescence signal at 520 nm and biotinylated on the 3' end to bind to streptavidin coated plates or beads in the immobilization phase.

Table 3. Selected Bacterial Sequences for Capture and Target Probes

V3 Sequence Region	DNA Capture Probe	RNA Target Probe
EC 447-467	5'-ATTAAC TTTACTCCCTTCCTC-3'	5'-GAGGAAGGGAGUAAAGUAAU-3'
EC 467-486	5' TAACGTCAATGAGCAAAGGT-3'	5'-ACCUUUGCUCAUUGACGUUA-3'

4.2.2 Platform Design

Streptavidin-coated 96 well plates and streptavidin-coated magnetic beads were both utilized as base platforms for immobilization. Biotinylated tagged-DNA is immobilized onto the streptavidin-coated plates or beads. Synthetic RNA is added and hybridized with ssDNA to form DNA/RNA duplex. DSN is then added to cleave ssDNA in the duplex. Following cleaving ssDNA, RNA is released back into solution. Unbound RNA hybridizes with a new immobilized DNA probe. Fluorescent labels released by DSN cleavage are collected for downstream detection.

4.2.3 Immobilization Protocol

Fluorescently labeled synthetic DNA capture probes (0-100 pmol) were immobilized on streptavidin coated beads or plates and incubated for 20 minutes at 20°C. At the start of the incubation, the initial baseline fluorescence signal emitted by the DNA probes were measured at 520 nm at each concentration using a microplate reader. After incubation, plates or beads were

washed 3x with buffer to remove the unbound capture probes. Bound capture probes were then measured again at 520nm using a microplate reader. The immobilization efficiency was measured as follows:

$$\text{Immobilization Efficiency (\%)} = \frac{\text{pmol DNA immobilized}}{\text{Initial pmol DNA}} \times 100$$

The immobilization efficiency was compared to the maximum available binding sites/concentration of the plates or beads to determine which DNA concentration was most optimal for using in the subsequent hybridization step.

4.2.4 Hybridization Protocol

Based on the optimal DNA probe concentration from the immobilization step, unlabeled synthetic ssDNA probes were then immobilized on beads or plates and incubated for 20 minutes at 20°C. Plates or beads were washed 3x with buffer to remove the unbound capture probes. Synthetic fluorescently labeled RNA target probes (0-50 pmol) were added to solution. Baseline fluorescent signals at 520 nm were measured from 0-50 pmol of RNA in solution at the beginning of the incubation period using a microplate reader. A hot start followed by incubation at 30 min at 45°C allowed for hybridization. Plates or beads were washed 3x with buffer to remove the unhybridized probes. Hybridized duplexes probes were then measured at 520nm using a microplate reader. The hybridization efficiency was measured as follows:

$$\text{Hybridization Efficiency (\%)} = \frac{\text{pmol RNA hybridized}}{\text{pmol DNA immobilized}} \times 100 \quad (5)$$

The hybridization efficiency was one of the tools to determine not only the optimal conditions for hybridization, but also to determine how much unhybridized DNA capture probes were available for target recycling after DSN was added.

4.2.5 DSN-mediated Target Recycling Protocol

Following optimization of the hybridization, DSN activity and target recycling was measured. Fluorescently labeled *ssDNA* probes were immobilized onto plates or beads and hybridized with unlabeled synthetic RNA probes as previously described. The expected concentrations of immobilized DNA and hybridized RNA were determined from the previous experiments and used here. DSN was added at different concentrations (0.02-0.1 units/ μ L) and incubated over different time periods (30-120 min). Concentration, temperature and time were key factors that were tested to optimize DSN activity. The solution was then washed 2-3x with buffer. The wash solution was collected as the fluorescent signal (cleaved, unbound, and tagged-DNA probes) was accumulated in this solution and could be pipetted into another well to measure the signal at 520 nm using a microplate reader. The measured fluorescence of the wash solution was incorporated into the amplification factor which was calculated as follows:

$$\text{Amplification Factor} = \frac{\text{DNA pmol in "wash solution"}}{\text{RNA pmol hybridized}}$$

4.3 Results and Discussion

4.3.1 Immobilization Efficiency

Immobilization efficiency of EC 447 and EC 467 probes on plates versus magnetic beads at varying concentrations from 0-100pmol DNA were compared. Results comparing initial concentration of DNA probe added versus bound (immobilized) DNA concentration is shown in Figure 19. Although EC447 DNA had a higher overall immobilization efficiency on the plates, the magnetic beads platform provided more DNA binding sites than the plates, ultimately making that the magnetic beads the preferred platform. Additional experiments showing the differences between EC447 DNA and EC467 DNA would have been useful for comparison,

however experiments described below will explain why those comparison experiments were not needed. Ultimately, immobilization was most optimal using EC 467 DNA probes on the magnetic bead platform (Figure 19).

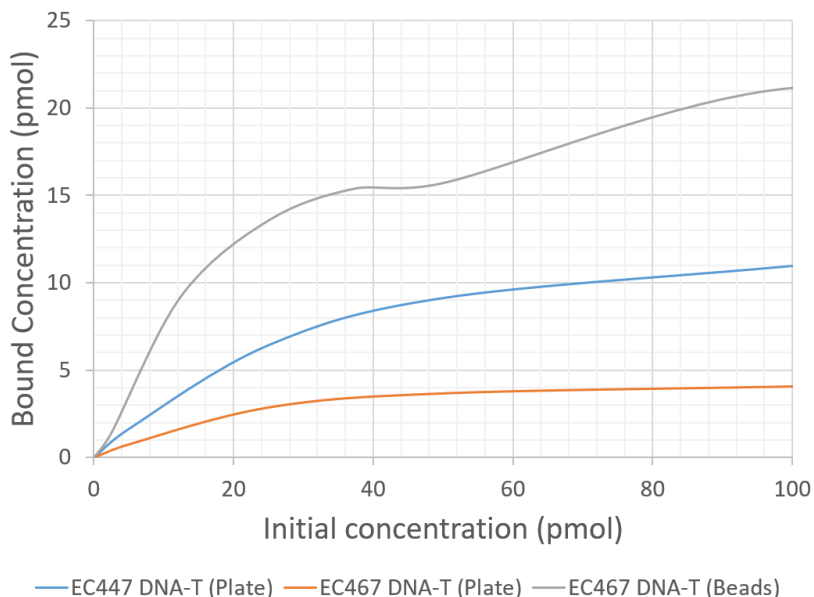


Figure 19. Comparison of plate and magnetic bead platform for ssDNA probe immobilization. DNA-T represents the ssDNA fluorescently tagged capture probes

4.3.2 Hybridization Efficiency

To observe the hybridization efficiency on the streptavidin-coated magnetic beads, EC 467 RNA probes (0-50 pmol) were added to previously immobilized EC467 DNA probes (initial concentration of 50 pmol). Figure 20 below shows hybridization efficiency at different initial RNA probe concentrations. The data shows that at an initial RNA concentration of ~12 pmol, the hybridization efficiency is ~29%. This means that ~71% of the immobilized DNA probes are unhybridized. By adding DSN at this RNA concentration, the RNA probes can theoretically undergo slightly more than 2 rounds of target recycling to exhaust all the uncleaved DNA probes. To demonstrate the feasibility of DSN, we utilized these DNA/RNA concentrations

providing this low, but reliable hybridization efficiency for subsequent experiments to observe multiple rounds of DSN-mediated target recycling.

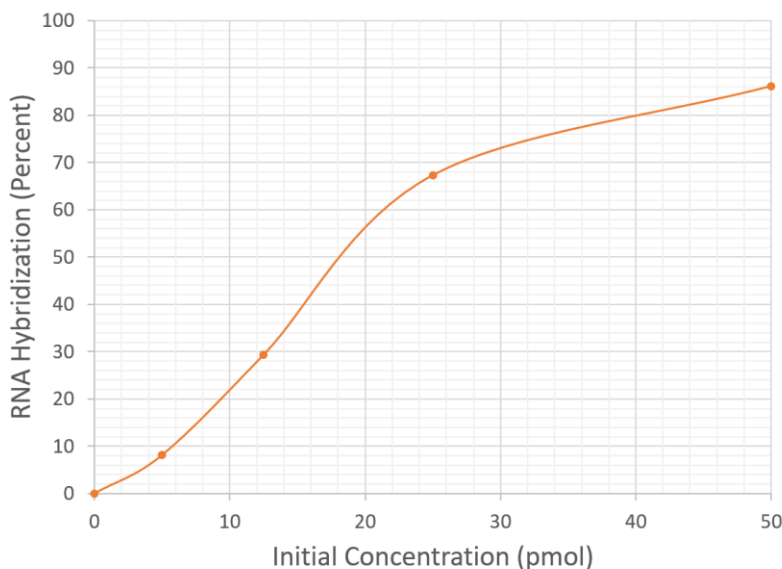


Figure 20. RNA hybridization efficiency of EC467 RNA on DNA immobilized beads. Hybridization efficiency improved with increasing initial concentrations of RNA.

This section briefly explains why EC 467 probes were utilized for the downstream DSN amplification. During hybridization experiments, both sets of probe sequences were tested and compared. After immobilization, 12.5pmol RNA (based on previous experiments) were added for hybridization to take place. The addition of EC447 RNA caused a significant drop in signal intensity in sample containing beads immobilized with EC447 DNA and was followed by a further drop in signal following hybridization and wash steps. Addition, hybridization, and washing of EC467 RNA caused minimal change in signal to sample containing beads immobilized with EC467 DNA. After looking more into the literature about assay conditions and sequence limitations, it was suspected that the prevalence of secondary structures (repeating G content) in EC 447 synthetic RNA inhibited hybridization efficiency and resulted in significant signal loss. This is illustrated in Figure 21 below. As a result of the instability and signal quenching of the

RNA:DNA duplex with the EC447 probes, EC467 probes were utilized for the remainder of the experiments.

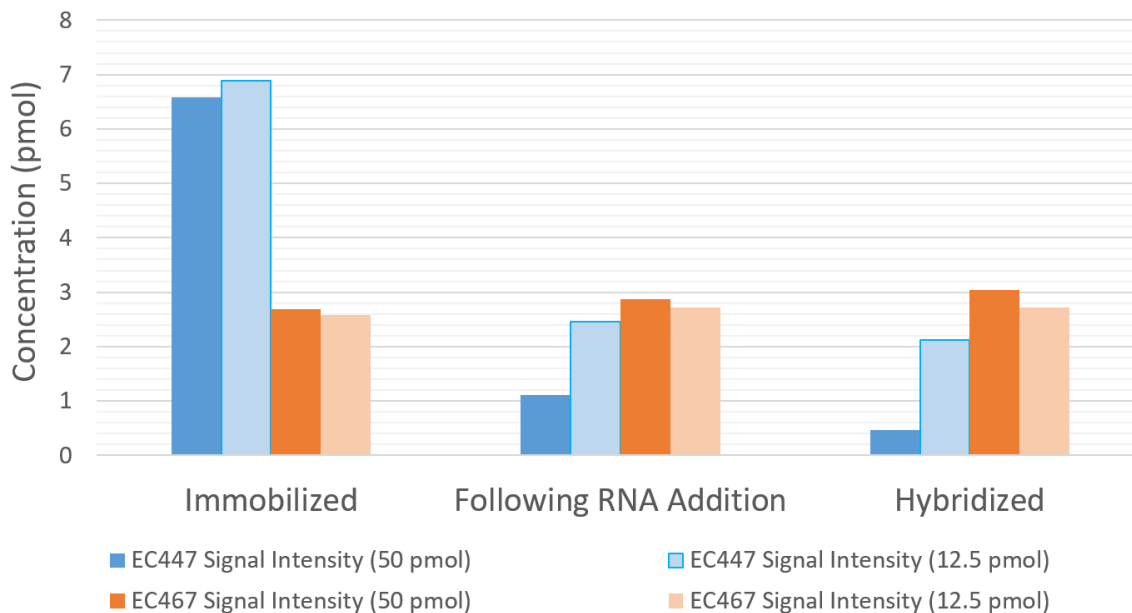


Figure 21. Comparison of fluorescence signal intensity before, during, and after addition of RNA probes.

4.3.3 Feasibility of DSN-mediated Strategy

After establishing a DNA and RNA probe concentration, the next step was to better understand DSN activity and feasibility for target recycling. Initially, DSN concentration and duration of enzyme digestion were tested to optimize the basic conditions of the experiment. Based on the melting temperature of the probes as well as information from the literature, 45 °C was used as the incubation temperature.

In Figure 22, the effect of adding of 0.02U/ μ L DSN at 45°C was measured every 30 minutes for 120 minutes. Change in signal was minimal over 120 min when compared to the baseline signal intensity from hybridization. The DSN amplification factor was calculated to be 1.66 after 2 hours.

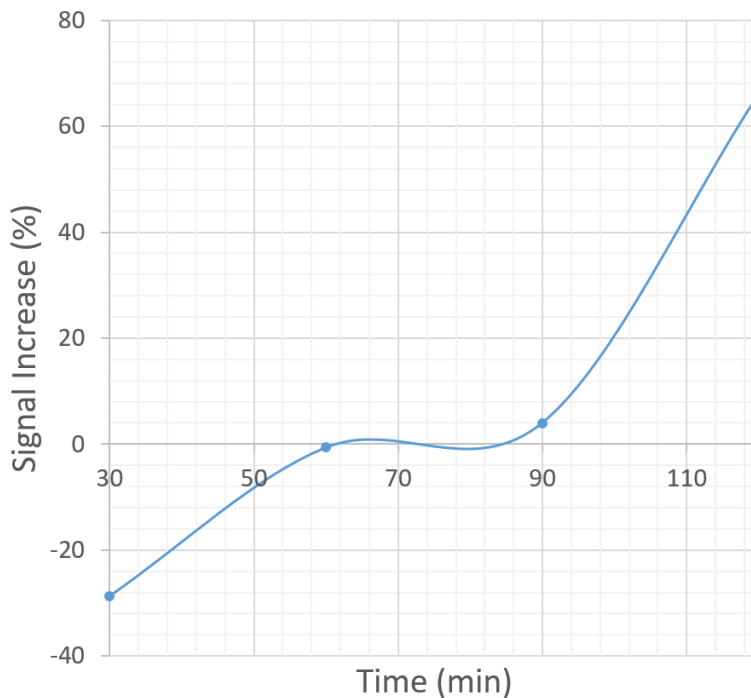


Figure 22. Change in signal intensity with the addition of 0.02U/ μ L DSN and incubation at 45°C as a function of time. Change in signal was minimal over 120 min when compared to the baseline signal intensity from hybridization.

To further test the effect of time on DSN activity, varying concentrations of DSN (of 0.02(1U), 0.05(2.5U), and 0.1U/ μ L(5U)) were added to the hybridized solution and measured at 60 and 120 min timepoints. As demonstrated in Figure 23, at each concentration, the increase in signal was minimal across the two time points. However, there appeared to be greater differences in signal increase between the concentrations. At 0.1U/ μ L concentration of DSN, a decrease in signal intensity was observed after incubation for 120 min.

These results show the feasibility of DSN cleavage towards sequences representative of bacterial rRNA and capability of RNA to rehybridize with uncleaved DNA probes. A major factor limiting DSN amplification is the immobilization platform as the low efficiency of DNA immobilization limits the ceiling of DSN amplification and remains a time and labor-intensive protocol. Therefore, further optimization of the assay conditions and platform is needed to increase the amplification factor.

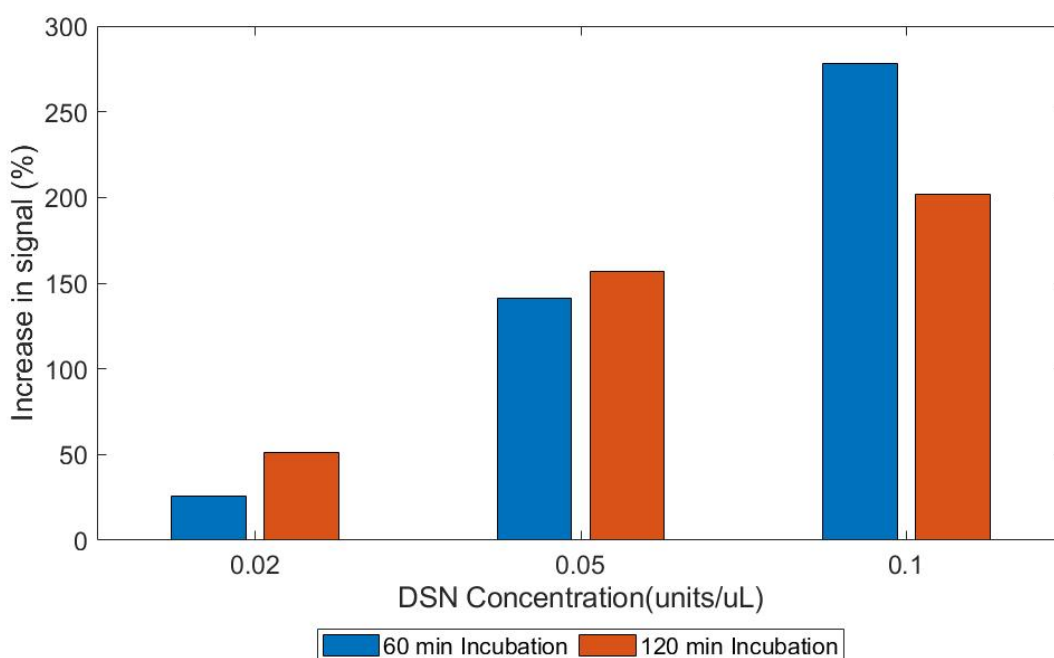


Figure 23. Change in signal intensity following incubation at 45°C with varying concentrations of DSN over time.

4.4. Conclusions

Major aspects of a DSN-mediated target recycling strategy have been described and demonstrated for signal amplification of target bacterial-based RNA sequences. In order to make this assay less labor intensive, provide real-time quantification, and reduce the amplification factor ceiling due to immobilization capacity, two potential avenues will be compared in the future work.

These strategies involve using a competitive DNA strand design approach and designing a molecular beacon (hairpin) probe. Additionally, real bacterial cell samples must be utilized to determine how effective the cell lysis process is in denaturing the secondary structures of 16S rRNA without compromising sequence integrity. Testing extracted RNA from these lysed samples with DSN will determine the true feasibility of this assay for bacterial detection. Finally, combining this DSN-mediated strategy with a short-term culture method will help to quantify the viable, infectious pathogens in water samples, making it a valuable tool in pathogen analysis and risk assessment. Furthermore, adapting this assay onto a centrifugal microfluidics platform will reduce time and labor while delivering automation that could improve the efficacy of the assay at the point-of-sample collection. The design will also allow for multiplex detection of different pathogens and/or performing the assay on different samples simultaneously. Figure 24 depicts CAD illustrations of a potential disc design implementing the major steps of the assay.

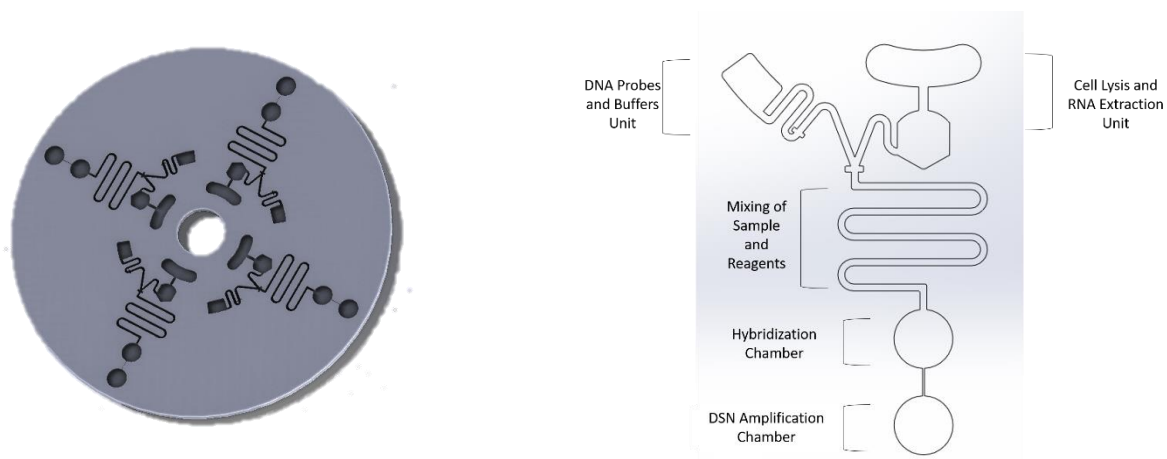


Figure 24. (Left) 3D depiction of CD while (Right) highlights 2D view with major units and steps of the assay specified.

CHAPTER 5:

CONCLUSIONS AND FUTURE WORK

Several limitations of water quality analysis have been identified and guided the work in this dissertation. Progress towards developing centrifugal based systems for improving speed, sensitivity, and accessibility of water quality detection has been demonstrated. A prototype centrifugal microfluidic platform performing a complete ddLAMP assay has been developed for detection of microbial contaminations in water. This disc coupled with the analysis instrument enables automation, rapid quantitative results, and portability which highlights its potential to be deployed for use in the field at the point-of-sample collection. More diverse environmental samples still require testing with the disc to optimize for real sample detection. Additionally, since variations in fabrication and manual assembly limit reproducibility in the lab, moving to large-scale manufacturing entities mitigate this challenge and provide more insight into optimizing the entire system for real world deployment.

Additionally, the integration of SAPs beads with the centrifugal microfluidic platform provides a solution to another major problem upstream of detection in water sample analysis: concentration. Our proof-of-concept sample concentration system can concentrate volumes on the millimeter scale, and its seamless integration with the disc creates a great potential in developing a totally integrated system, especially if a downstream detection design is implemented on the same disc.

Furthermore, the last major step in water analysis is risk assessment based on the results of the detection assay. The ability to quickly and effectively determine the pathogen diversity, viability, infectivity in water samples is an on-going challenge in the field. Developing the

DSN-mediated target recycling assay targeting rRNA in bacteria coupled is extremely useful with regards to downstream viability assessment. Combining this strategy with a modified culture-based assay and subsequent incorporation of the assay onto the disc platform has the potential to be a very useful tool at the point-of-sample collection.

Overall, this work aims to show the advantages of centrifugal microfluidic-based point-of-sample collection platforms, demonstrate proof-of-concept systems and remaining challenges, and highlights the future work focused on achieving a totally integrated system for microbial water quality analysis. The implementation of these systems in both developing and developed areas will streamline water quality analysis, keep communities informed in a timely manner, and mitigate risks to public health.

Bibliography

Approved CWA Microbiological Test Methods / US EPA. US EPA. (2020).

<https://www.epa.gov/cwa-methods/approved-cwa-microbiological-test-methods>.

Baymiev, A., Baymiev, A., Kuluev, B., Shvets, K., Yamidanov, R., & Matniyazov, R. et al. (2020). Modern Approaches to Differentiation of Live and Dead Bacteria Using Selective Amplification of Nucleic Acids. *Microbiology*, 89(1), 13-27.

<https://doi.org/10.1134/s0026261720010038>

Bleve, G., Rizzotti, L., Dellaglio, F., & Torriani, S. (2003). Development of Reverse Transcription (RT)-PCR and Real-Time RT-PCR Assays for Rapid Detection and Quantification of Viable Yeasts and Molds Contaminating Yogurts and Pasteurized Food Products. *Applied And Environmental Microbiology*, 69(7), 4116-4122. <https://doi.org/10.1128/aem.69.7.4116-4122.2003>

Bowsher, A., Kearns, P., & Shade, A. (2019). 16S rRNA/rRNA Gene Ratios and Cell Activity Staining Reveal Consistent Patterns of Microbial Activity in Plant-Associated Soil. *Msystems*, 4(2). <https://doi.org/10.1128/msystems.00003-19>

Bridle, H., Balharry, D., Gaiser, B., & Johnston, H. (2015). Exploitation of Nanotechnology for the Monitoring of Waterborne Pathogens: State-of-the-Art and Future Research Priorities. *Environmental Science & Technology*, 49(18), 10762-10777.

<https://doi.org/10.1021/acs.est.5b01673>

Byappanahalli, M., Nevers, M., Korajkic, A., Staley, Z., & Harwood, V. (2012). Enterococci in the Environment. *Microbiology And Molecular Biology Reviews*, 76(4), 685-706.

<https://doi.org/10.1128/mmbr.00023-12>

Cho, Y., Lee, J., Park, J., Lee, B., Lee, Y., & Ko, C. (2007). One-step pathogen specific DNA extraction from whole blood on a centrifugal microfluidic device. *Lab On A Chip*, 7(5), 565.

<https://doi.org/10.1039/b616115d>

Digital Droplet PCR Applications Guide. Bio-rad.com. (2020). Retrieved 31 December 2020, from https://www.bio-rad.com/webroot/web/pdf/lsr/literature/Bulletin_6407.pdf.

Digital PCR: A Technical Guide To PCR Technologies. Sigmaaldrich.com. (2020).

<https://www.sigmaaldrich.com/technical-documents/articles/biology/digital-pcr.html>.

Duarte, C., Salm, E., Dorvel, B., Reddy, B., & Bashir, R. (2013). On-chip parallel detection of foodborne pathogens using loop-mediated isothermal amplification. *Biomedical Microdevices*, 15(5), 821-830. <https://doi.org/10.1007/s10544-013-9769-5>

Duffy, E., Padovani, R., He, X., Gorkin, R., Vereshchagina, E., & Ducrée, J. et al. (2017). New strategies for stationary phase integration within centrifugal microfluidic platforms for

applications in sample preparation and pre-concentration. *Analytical Methods*, 9(13), 1998-2006. <https://doi.org/10.1039/c7ay00127d>

Duffy, G., Maguire, I., Heery, B., Gers, P., Ducreé, J., & Regan, F. (2018). ChromiSense: A colourimetric lab-on-a-disc sensor for chromium speciation in water. *Talanta*, 178, 392-399. <https://doi.org/10.1016/j.talanta.2017.09.066>

Duffy, G., Maguire, I., Heery, B., Nwankire, C., Ducreé, J., & Regan, F. (2017). PhosphaSense: A fully integrated, portable lab-on-a-disc device for phosphate determination in water. *Sensors And Actuators B: Chemical*, 246, 1085-1091. <https://doi.org/10.1016/j.snb.2016.12.040>

Frickmann, H., Zautner, A., Moter, A., Kikhney, J., Hagen, R., Stender, H., & Poppert, S. (2017). Fluorescence in situ hybridization (FISH) in the microbiological diagnostic routine laboratory: a review. *Critical Reviews In Microbiology*, 43(3), 263-293. <https://doi.org/10.3109/1040841x.2016.1169990>

Gerasimova, Y., & Kolpashchikov, D. (2014). Enzyme-assisted target recycling (EATR) for nucleic acid detection. *Chem. Soc. Rev.*, 43(17), 6405-6438. <https://doi.org/10.1039/c4cs00083h>

Halford, C., Gau, V., Churchill, B., & Haake, D. (2013). Bacterial Detection & Identification Using Electrochemical Sensors. *Journal Of Visualized Experiments*, (74). <https://doi.org/10.3791/4282>

Hindson, B., Ness, K., Masquelier, D., Belgrader, P., Heredia, N., & Makarewicz, A. et al. (2011). High-Throughput Droplet Digital PCR System for Absolute Quantitation of DNA Copy Number. *Analytical Chemistry*, 83(22), 8604-8610. <https://doi.org/10.1021/ac202028g>

Huang, J., Shangguan, J., Guo, Q., Ma, W., Wang, H., & Jia, R. et al. (2019). Colorimetric and fluorescent dual-mode detection of microRNA based on duplex-specific nuclease assisted gold nanoparticle amplification. *The Analyst*, 144(16), 4917-4924. <https://doi.org/10.1039/c9an01013k>

James, G. (2010). Universal Bacterial Identification by PCR and DNA Sequencing of 16S rRNA Gene. *PCR For Clinical Microbiology*, 209-214. https://doi.org/10.1007/978-90-481-9039-3_28

Janda, J., & Abbott, S. (2007). 16S rRNA Gene Sequencing for Bacterial Identification in the Diagnostic Laboratory: Pluses, Perils, and Pitfalls. *Journal Of Clinical Microbiology*, 45(9), 2761-2764. <https://doi.org/10.1128/jcm.01228-07>

Jofre, J., & Blanch, A. (2010). Feasibility of methods based on nucleic acid amplification techniques to fulfil the requirements for microbiological analysis of water quality. *Journal Of Applied Microbiology*, 109(6), 1853-1867. <https://doi.org/10.1111/j.1365-2672.2010.04830.x>

Kato, H., Yoshida, A., Ansai, T., Watari, H., Notomi, T., & Takehara, T. (2007). Loop-mediated isothermal amplification method for the rapid detection of *Enterococcus faecalis* in infected root canals. *Oral Microbiology And Immunology*, 22(2), 131-135. <https://doi.org/10.1111/j.1399-302x.2007.00328.x>

- Kido, H., Micic, M., Smith, D., Zoval, J., Norton, J., & Madou, M. (2007). A novel, compact disk-like centrifugal microfluidics system for cell lysis and sample homogenization. *Colloids And Surfaces B: Biointerfaces*, 58(1), 44-51. <https://doi.org/10.1016/j.colsurfb.2007.03.015>
- Kim, E., Howes, P., Crowder, S., & Stevens, M. (2016). Multi-Amplified Sensing of MicroRNA by a Small DNA Fragment-Driven Enzymatic Cascade Reaction. *ACS Sensors*, 2(1), 111-118. <https://doi.org/10.1021/acssensors.6b00601>
- Kinahan, D., Julius, L., Schoen, C., Dreo, T., & Ducree, J. (2018). Automated DNA purification and multiplexed lamp assay preparation on a centrifugal microfluidic “Lab-on-a-Disc” platform. *2018 IEEE Micro Electro Mechanical Systems (MEMS)*. <https://doi.org/10.1109/memsys.2018.8346761>
- Ko, J., & Yoo, J. (2018). Loop-Mediated Isothermal Amplification Using a Lab-on-a-Disc Device with Thin-film Phase Change Material. *Applied Biochemistry And Biotechnology*, 186(1), 54-65. <https://doi.org/10.1007/s12010-018-2720-8>
- Kolm, C., Martzy, R., Brunner, K., Mach, R., Krska, R., & Heinze, G. et al. (2017). A Complementary Isothermal Amplification Method to the U.S. EPA Quantitative Polymerase Chain Reaction Approach for the Detection of Enterococci in Environmental Waters. *Environmental Science & Technology*, 51(12), 7028-7035. <https://doi.org/10.1021/acs.est.7b01074>
- Kong, L., Perebikovskiy, A., Moebius, J., Kulinsky, L., & Madou, M. (2016). Lab-on-a-CD. *Journal Of Laboratory Automation*, 21(3), 323-355. <https://doi.org/10.1177/2211068215588456>
- Lebaron, P., Henry, A., Lepeuple, A., Pena, G., & Servais, P. (2005). An operational method for the real-time monitoring of E. coli numbers in bathing waters. *Marine Pollution Bulletin*, 50(6), 652-659. <https://doi.org/10.1016/j.marpolbul.2005.01.016>
- Li, Y., Zhang, J., Zhao, J., Zhao, L., Cheng, Y., & Li, Z. (2016). A simple molecular beacon with duplex-specific nuclease amplification for detection of microRNA. *The Analyst*, 141(3), 1071-1076. <https://doi.org/10.1039/c5an02312b>
- Liu, D., Liang, G., Zhang, Q., & Chen, B. (2013). Detection of Mycobacterium tuberculosis Using a Capillary-Array Microsystem with Integrated DNA Extraction, Loop-Mediated Isothermal Amplification, and Fluorescence Detection. *Analytical Chemistry*, 85(9), 4698-4704. <https://doi.org/10.1021/ac400412m>
- Liu, L., Gao, Y., Liu, H., & Xia, N. (2015). An ultrasensitive electrochemical miRNAs sensor based on miRNAs-initiated cleavage of DNA by duplex-specific nuclease and signal amplification of enzyme plus redox cycling reaction. *Sensors And Actuators B: Chemical*, 208, 137-142. <https://doi.org/10.1016/j.snb.2014.11.023>
- Lu, L., Yang, B., & Kang, T. (2017). A dual amplification strategy for ultrasensitive detection of microRNA. *Applied Surface Science*, 426, 597-604. <https://doi.org/10.1016/j.apsusc.2017.07.091>

- M.J.A.D., Zohourian, and K. Kabiri. (2008) "Superabsorbent Polymer Materials: A Review". *Iranian Polymer Journal*, 17(6), 451-477.
https://www.researchgate.net/publication/242582443_Superabsorbent_Polymer_Materials_A_Review
- Maguire, I., Fitzgerald, J., McPartlin, D., Heery, B., Murphy, C., & Nwankire, C. et al. (2017). A centrifugal microfluidic-based approach for multi-toxin detection for real-time marine water-quality monitoring. *OCEANS 2017 - Aberdeen*. <https://doi.org/10.1109/oceanse.2017.8084975>
- Maguire, I., O'Kennedy, R., Ducreé, J., & Regan, F. (2018). A review of centrifugal microfluidics in environmental monitoring. *Analytical Methods*, 10(13), 1497-1515.
<https://doi.org/10.1039/c8ay00361k>
- Medlin, L., Elwood, H., Stickel, S., & Sogin, M. (1988). The characterization of enzymatically amplified eukaryotic 16S-like rRNA-coding regions. *Gene*, 71(2), 491-499.
[https://doi.org/10.1016/0378-1119\(88\)90066-2](https://doi.org/10.1016/0378-1119(88)90066-2)
- Mendes Silva, D., & Domingues, L. (2015). On the track for an efficient detection of *Escherichia coli* in water: A review on PCR-based methods. *Ecotoxicology And Environmental Safety*, 113, 400-411. <https://doi.org/10.1016/j.ecoenv.2014.12.015>
- Meng, X., Zhu, Y., Chen, Y., Lu, Y., Xu, Y., & Cheng, J. (2017). Conditional siphon priming for multi-step assays on centrifugal microfluidic platforms. *Sensors And Actuators B: Chemical*, 242, 710-717. <https://doi.org/10.1016/j.snb.2016.11.063>
- Odonkor, S., & Ampofo, J. (2013). *Escherichia coli* as an indicator of bacteriological quality of water: an overview. *Microbiology Research*, 4(1), 2. <https://doi.org/10.4081/mr.2013.e2>
- Other Clean Water Act Test Methods: Microbiological | US EPA*. US EPA. (2020).
<https://www.epa.gov/cwa-methods/other-clean-water-act-test-methods-microbiological>.
- Peng, W., Zhao, Q., Piao, J., Zhao, M., Huang, Y., & Zhang, B. et al. (2018). Ultra-sensitive detection of microRNA-21 based on duplex-specific nuclease-assisted target recycling and horseradish peroxidase cascading signal amplification. *Sensors And Actuators B: Chemical*, 263, 289-297. <https://doi.org/10.1016/j.snb.2018.02.143>
- Pinheiro, L., Coleman, V., Hindson, C., Herrmann, J., Hindson, B., Bhat, S., & Emslie, K. (2011). Evaluation of a Droplet Digital Polymerase Chain Reaction Format for DNA Copy Number Quantification. *Analytical Chemistry*, 84(2), 1003-1011.
<https://doi.org/10.1021/ac202578x>
- Platts-Mills, J., Operario, D., & Houpt, E. (2011). Molecular Diagnosis of Diarrhea: Current Status and Future Potential. *Current Infectious Disease Reports*, 14(1), 41-46.
<https://doi.org/10.1007/s11908-011-0223-7>
- Qiu, X., Zhang, H., Yu, H., Jiang, T., & Luo, Y. (2015). Duplex-specific nuclease-mediated bioanalysis. *Trends In Biotechnology*, 33(3), 180-188.
<https://doi.org/10.1016/j.tibtech.2014.12.008>

- Quan, P., Sauzade, M., & Brouzes, E. (2018). dPCR: A Technology Review. *Sensors*, *18*(4), 1271. <https://doi.org/10.3390/s18041271>
- Rajapaksha, P., Elbourne, A., Gangadoo, S., Brown, R., Cozzolino, D., & Chapman, J. (2019). A review of methods for the detection of pathogenic microorganisms. *The Analyst*, *144*(2), 396-411. <https://doi.org/10.1039/c8an01488d>
- Ramírez-Castillo, F., Loera-Muro, A., Jacques, M., Garneau, P., Avelar-González, F., Harel, J., & Guerrero-Barrera, A. (2015). Waterborne Pathogens: Detection Methods and Challenges. *Pathogens*, *4*(2), 307-334. <https://doi.org/10.3390/pathogens4020307>
- Safavieh, M., Kanakasabapathy, M., Tarlan, F., Ahmed, M., Zourob, M., Asghar, W., & Shafiee, H. (2016). Emerging Loop-Mediated Isothermal Amplification-Based Microchip and Microdevice Technologies for Nucleic Acid Detection. *ACS Biomaterials Science & Engineering*, *2*(3), 278-294. <https://doi.org/10.1021/acsbiomaterials.5b00449>
- Sanders, R., Huggett, J., Bushell, C., Cowen, S., Scott, D., & Foy, C. (2011). Evaluation of Digital PCR for Absolute DNA Quantification. *Analytical Chemistry*, *83*(17), 6474-6484. <https://doi.org/10.1021/ac103230c>
- Santiago-Felipe, S., Tortajada-Genaro, L., Carrascosa, J., Puchades, R., & Maquieira, Á. (2016). Real-time loop-mediated isothermal DNA amplification in compact disc micro-reactors. *Biosensors And Bioelectronics*, *79*, 300-306. <https://doi.org/10.1016/j.bios.2015.12.045>
- Sayad, A., Ibrahim, F., Uddin, S., Pei, K., Mohktar, M., Madou, M., & Thong, K. (2016). A microfluidic lab-on-a-disc integrated loop mediated isothermal amplification for foodborne pathogen detection. *Sensors And Actuators B: Chemical*, *227*, 600-609. <https://doi.org/10.1016/j.snb.2015.10.116>
- Schuler, F., Schwemmer, F., Trotter, M., Wadle, S., Zengerle, R., von Stetten, F., & Paust, N. (2015). Centrifugal step emulsification applied for absolute quantification of nucleic acids by digital droplet RPA. *Lab On A Chip*, *15*(13), 2759-2766. <https://doi.org/10.1039/c5lc00291e>
- Schuler, F., Trotter, M., Geltman, M., Schwemmer, F., Wadle, S., & Domínguez-Garrido, E. et al. (2016). Digital droplet PCR on disk. *Lab On A Chip*, *16*(1), 208-216. <https://doi.org/10.1039/c5lc01068c>
- Seo, J., Park, B., Oh, S., Choi, G., Kim, D., Lee, E., & Seo, T. (2017). Development of a high-throughput centrifugal loop-mediated isothermal amplification microdevice for multiplex foodborne pathogenic bacteria detection. *Sensors And Actuators B: Chemical*, *246*, 146-153. <https://doi.org/10.1016/j.snb.2017.02.051>
- Shagin, D. (2002). A Novel Method for SNP Detection Using a New Duplex-Specific Nuclease From Crab Hepatopancreas. *Genome Research*, *12*(12), 1935-1942. <https://doi.org/10.1101/gr.547002>
- Shen, F., Sun, B., Kreutz, J., Davydova, E., Du, W., & Reddy, P. et al. (2011). Multiplexed Quantification of Nucleic Acids with Large Dynamic Range Using Multivolume Digital RT-

PCR on a Rotational SlipChip Tested with HIV and Hepatitis C Viral Load. *Journal Of The American Chemical Society*, 133(44), 17705-17712. <https://doi.org/10.1021/ja2060116>

Shi, C., Li, S., Chen, Z., Liu, Q., & Yu, R. (2018). Label-Free and Multiplexed Quantification of microRNAs by Mass Spectrometry Based on Duplex-Specific-Nuclease-Assisted Recycling Amplification. *Analytical Chemistry*, 91(3), 2120-2127. <https://doi.org/10.1021/acs.analchem.8b04583>

Sia, S., & Kricka, L. (2008). Microfluidics and point-of-care testing. *Lab On A Chip*, 8(12), 1982. <https://doi.org/10.1039/b817915h>

Smith, S., Mager, D., Perebikovskiy, A., Shamloo, E., Kinahan, D., & Mishra, R. et al. (2016). CD-Based Microfluidics for Primary Care in Extreme Point-of-Care Settings. *Micromachines*, 7(2), 22. <https://doi.org/10.3390/mi7020022>

Stadhouders, R., Pas, S., Anber, J., Voermans, J., Mes, T., & Schutten, M. (2010). The Effect of Primer-Template Mismatches on the Detection and Quantification of Nucleic Acids Using the 5' Nuclease Assay. *The Journal Of Molecular Diagnostics*, 12(1), 109-117. <https://doi.org/10.2353/jmoldx.2010.090035>

Stevens, K., & Jaykus, L. (2004). Bacterial Separation and Concentration from Complex Sample Matrices: A Review. *Critical Reviews In Microbiology*, 30(1), 7-24. <https://doi.org/10.1080/10408410490266410>

Strohmeier, O., Emperle, A., Roth, G., Mark, D., Zengerle, R., & von Stetten, F. (2013). Centrifugal gas-phase transition magnetophoresis (GTM) – a generic method for automation of magnetic bead based assays on the centrifugal microfluidic platform and application to DNA purification. *Lab Chip*, 13(1), 146-155. <https://doi.org/10.1039/c2lc40866j>

Strohmeier, O., Keller, M., Schwemmer, F., Zehnle, S., Mark, D., & von Stetten, F. et al. (2015). Centrifugal microfluidic platforms: advanced unit operations and applications. *Chemical Society Reviews*, 44(17), 6187-6229. <https://doi.org/10.1039/c4cs00371c>

Tang, M., Wang, G., Kong, S., & Ho, H. (2016). A Review of Biomedical Centrifugal Microfluidic Platforms. *Micromachines*, 7(2), 26. <https://doi.org/10.3390/mi7020026>

Tao, Y., Yin, D., Jin, M., Fang, J., Dai, T., & Li, Y. et al. (2017). Double-loop hairpin probe and doxorubicin-loaded gold nanoparticles for the ultrasensitive electrochemical sensing of microRNA. *Biosensors And Bioelectronics*, 96, 99-105. <https://doi.org/10.1016/j.bios.2017.04.040>

Tourlousse, D., Ahmad, F., Stedtfeld, R., Seyrig, G., Tiedje, J., & Hashsham, S. (2012). A polymer microfluidic chip for quantitative detection of multiple water- and foodborne pathogens using real-time fluorogenic loop-mediated isothermal amplification. *Biomedical Microdevices*, 14(4), 769-778. <https://doi.org/10.1007/s10544-012-9658-3>

- van Seventer, J., & Hochberg, N. (2017). Principles of Infectious Diseases: Transmission, Diagnosis, Prevention, and Control. *International Encyclopedia Of Public Health*, 22-39. <https://doi.org/10.1016/b978-0-12-803678-5.00516-6>
- Váradi, L., Luo, J., Hibbs, D., Perry, J., Anderson, R., Orenge, S., & Groundwater, P. (2017). Methods for the detection and identification of pathogenic bacteria: past, present, and future. *Chemical Society Reviews*, 46(16), 4818-4832. <https://doi.org/10.1039/c6cs00693k>
- Wang, Q., Li, R., Yin, B., & Ye, B. (2015). Colorimetric detection of sequence-specific microRNA based on duplex-specific nuclease-assisted nanoparticle amplification. *The Analyst*, 140(18), 6306-6312. <https://doi.org/10.1039/c5an01350j>
- Wang, Y., Howes, P., Kim, E., Spicer, C., Thomas, M., & Lin, Y. et al. (2018). Duplex-Specific Nuclease-Amplified Detection of MicroRNA Using Compact Quantum Dot–DNA Conjugates. *ACS Applied Materials & Interfaces*, 10(34), 28290-28300. <https://doi.org/10.1021/acsami.8b07250>
- Water supply, sanitation and hygiene monitoring. World Health Organization.* (2020). https://www.who.int/water_sanitation_health/monitoring/coverage/en/.
- Wu, X., Huang, X., Zhu, Y., Li, J., & Hoffmann, M. (2020). Synthesis and application of superabsorbent polymer microspheres for rapid concentration and quantification of microbial pathogens in ambient water. *Separation And Purification Technology*, 239, 116540. <https://doi.org/10.1016/j.seppur.2020.116540>
- Wu, Y., He, Y., Yang, X., Yuan, R., & Chai, Y. (2018). A novel recyclable surface-enhanced Raman spectroscopy platform with duplex-specific nuclease signal amplification for ultrasensitive analysis of microRNA 155. *Sensors And Actuators B: Chemical*, 275, 260-266. <https://doi.org/10.1016/j.snb.2018.08.057>
- Xia, Y., Liu, Z., Yan, S., Yin, F., Feng, X., & Liu, B. (2016). Identifying multiple bacterial pathogens by loop-mediated isothermal amplification on a rotate & react slipchip. *Sensors And Actuators B: Chemical*, 228, 491-499. <https://doi.org/10.1016/j.snb.2016.01.074>
- Xie, X., Bahnemann, J., Wang, S., Yang, Y., & Hoffmann, M. (2016). “Nanofiltration” Enabled by Super-Absorbent Polymer Beads for Concentrating Microorganisms in Water Samples. *Scientific Reports*, 6(1). <https://doi.org/10.1038/srep20516>
- Xu, F., Dong, H., Cao, Y., Lu, H., Meng, X., & Dai, W. et al. (2016). Ultrasensitive and Multiple Disease-Related MicroRNA Detection Based on Tetrahedral DNA Nanostructures and Duplex-Specific Nuclease-Assisted Signal Amplification. *ACS Applied Materials & Interfaces*, 8(49), 33499-33505. <https://doi.org/10.1021/acsami.6b12214>
- Xu, F., Luo, L., Shi, H., He, X., Lei, Y., & Tang, J. et al. (2018). Label-free and sensitive microRNA detection based on a target recycling amplification-integrated superlong poly(thymine)-hosted copper nanoparticle strategy. *Analytica Chimica Acta*, 1010, 54-61. <https://doi.org/10.1016/j.aca.2018.01.010>

- Yan, H., Zhu, Y., Zhang, Y., Wang, L., Chen, J., & Lu, Y. et al. (2017). Multiplex detection of bacteria on an integrated centrifugal disk using bead-beating lysis and loop-mediated amplification. *Scientific Reports*, 7(1). <https://doi.org/10.1038/s41598-017-01415-x>
- Yilmaz, L., Ökten, H., & Noguera, D. (2006). Making All Parts of the 16S rRNA of *Escherichia coli* Accessible In Situ to Single DNA Oligonucleotides. *Applied And Environmental Microbiology*, 72(1), 733-744. <https://doi.org/10.1128/aem.72.1.733-744.2006>
- Ying, N., Ju, C., Sun, X., Li, L., Chang, H., & Song, G. et al. (2017). Lateral flow nucleic acid biosensor for sensitive detection of microRNAs based on the dual amplification strategy of duplex-specific nuclease and hybridization chain reaction. *PLOS ONE*, 12(9), e0185091. <https://doi.org/10.1371/journal.pone.0185091>
- Yuan, H., Chao, Y., & Shum, H. (2020). Droplet and Microchamber-Based Digital Loop-Mediated Isothermal Amplification (dLAMP). *Small*, 16(9), 1904469. <https://doi.org/10.1002/smll.201904469>
- Zhang, H., Fan, M., Jiang, J., Shen, Q., Cai, C., & Shen, J. (2019). Sensitive electrochemical biosensor for MicroRNAs based on duplex-specific nuclease-assisted target recycling followed with gold nanoparticles and enzymatic signal amplification. *Analytica Chimica Acta*, 1064, 33-39. <https://doi.org/10.1016/j.aca.2019.02.060>
- Zhang, S., Liu, R., Xing, Z., Zhang, S., & Zhang, X. (2016). Multiplex miRNA assay using lanthanide-tagged probes and the duplex-specific nuclease amplification strategy. *Chemical Communications*, 52(99), 14310-14313. <https://doi.org/10.1039/c6cc08334j>
- Zhu, Y., Chen, Y., Meng, X., Wang, J., Lu, Y., Xu, Y., & Cheng, J. (2017). Comprehensive Study of the Flow Control Strategy in a Wirelessly Charged Centrifugal Microfluidic Platform with Two Rotation Axes. *Analytical Chemistry*, 89(17), 9315-9321. <https://doi.org/10.1021/acs.analchem.7b02080>